TRENDS IN SCIENCES 2026; 23(6): 12525
https://doi.org/10.48048/tis.2026.12525
REVIEW ARTICLE

# Review on Recent Advances in Metal-substitution Modify Cobalt Ferrite Nanoparticles as Antibacterial Applications

**Retna Arilasita[1,3], Nurdiyantoro Putra Prasetya[3], Utari[1], Suharno[2], Riyatun[1] and Budi Purnama[1,*]**

*[1]Department of Physics, Faculty of Mathematics and Natural Sciences, Universitas Sebelas Maret, Surakarta 57126, Indonesia*
*[2]Department of Physics Education, Faculty of Teacher Training and Education, Universitas Sebelas Maret, Surakarta 57126, Indonesia*
*[3]Department of Physics, Faculty of Mathematics and Natural Sciences, Universitas Tanjungpura, Pontianak 78124, Indonesia*

**([*]Corresponding author's e-mail: bpurnama@mipa.uns.ac.id)**

*Received: 4 November 2025, Revised: 13 December 2025, Accepted: 20 December 2025, Published: 30 January 2026*

**Abstract**

In recent decades, the modification of magnetic nanoparticles-cobalt ferrite (NPM-cobalt ferrite) for antibacterial agents has been widely studied. These NPM-cobalt ferrites have unique characteristics, making them a viable option for the development of antibacterial agents. This paper presents a thorough analysis of the metal used to modify of cobalt ferrite in order to enhance antibacterial activity. Furthermore, this review delves into the antibacterial processes of cobalt ferrite, which are contingent upon critical characteristics including particle size, surface area, and ion replacement. The key findings of this review highlight the antibacterial performance of NPM-metal-cobalt ferrite based on the zone of inhibition (ZOI) and the standard percentages. However, it is important to carry out further investigate to optimize its activity. One of which is utilizing other metal elements that have not been utilized by looking at important parameter aspects in the results reported in this paper. This review contributes to the understanding and potential utilization of NPM-cobalt ferrite as an approach that is suitable for antibacterial agents.

**Keywords:** Antibacterial, Cobalt ferrite, Metal-cobalt ferrite, Nanoparticles, ZOI, Surface area, Structural properties

## Introduction

In recent years, several bacterially-induced diseases have resurfaced as a major global health concern, generating significant morbidity and mortality. The emergence of bacterial strains that are resistant to several drugs has presented new difficulties for the healthcare sector, necessitating the urgent development of novel and potent antibacterial treatment. This issue has been tackled using a number of approaches, including the application of nanotechnology. In this context, nanoparticles have attracted great attention due to their unique properties at the nano order scale, which allow them to interact more effectively with bacterial cells compared to bulk materials [1,2].

Several nanoparticles have been explored as antibacterial materials, one of which is a promising candidate is cobalt ferrite (CFO) nanoparticles. The combination of unique structural, magnetic, and chemical properties, along with a simple fabrication procedure, makes it excellent for application as antibacterial materials. In general, cobalt ferrite is a magnetic material with an inverse spinel structure and a number of advantageous characteristics. Its nano-scale size, less than 100 nm, causes a significant increase in the surface area to volume ratio, allowing for more effective contact with bacterial membranes [3]. Since there is a more noteworthy ratio of surface area to volume, nanoparticles (NPs) of smaller sizes are more

reactive. Therefore, the microbial application resulting from the synthesis of the cobalt ferrite must have a nanometer unit size. The surface shape of nanoparticles also acts as an antimicrobial, and an open bond is helpful for binding oxygen so that microbes will die [4]. Its elemental properties make it non-toxic and biodegradable [5]. Furthermore, their magnetic effects can be directed and utilized to penetrate and destroy biofilms. Functionalization of magnetic nanoparticles is crucial for efficient capture of the target [6].

Cobalt ferrite nanoparticles exhibit strong antibacterial properties, making them effective against a wide range of bacterial pathogens. There are 3 main mechanisms in antibacterial activity, namely adsorption, diffusion, and antibiofilm [7]. The adsorption mechanism utilizes nanoscale size with a large surface area to inhibit bacterial growth. Treatments that can change the size of a material include annealing temperature and metal ion substitution (metal type or concentration) [8-10]. Nevertheless, several studies have shown that the size of nanoparticles is not the main determinant of antibacterial activity. In such cases, other mechanisms, such as diffusion, play a role. These metal ions' interactions can result in a Fenton reaction, which both inactivates the enzyme proteins and serves as a precursor to the generation of ROS. Consequently, metal ion substitution is one potential way to increase the antibacterial activity of cobalt ferrite nanoparticles.

Metal substitution into the cobalt ferrite lattice can affect its structural, morphological, and magnetic properties. According to Kumar *et al.* [11] when the concentration of aluminum increases, aluminum-doped cobalt ferrite can decrease the crystallite size from 36.87 to 10.54 nm. Ion $Sm^{3+}$ substitution causes the distribution of cations where some tetrahedral $Fe^{3+}$ ions move towards the octahedral (B) site due to the replacement of $Fe^{3+}$ ions with $Sm^{3+}$ ions [12]. This affects the magnetic properties of the nanoparticles. Additional research has demonstrated that substituting different ions for rare earth metals can result in cation rearrangement and grain size changes, both of which have a major impact on cobalt ferrite's coercivity [13]. This analysis demonstrates that a key factor in metal substitution is the development of characteristics that permit usage as antibacterial materials.

This paper will review several research papers on magnetic nanoparticles-cobalt ferrite (NPM-CFO) applied as antimicrobial materials, whether pure NPM-CFO or substituted with other metals. It will also describe the synthesis of NPM-CFO, which produces tiny particle sizes, as needed as an antibacterial. Important factors influencing the effectiveness of biomedical applications of NPM-cobalt ferrite are biocompatibility and surface functionality. Particle size is one of the benchmarks for the success of the NPM-CFO synthesis process. Magnetic properties are sometimes not reported by researchers, even though these magnetic properties are the advantages of NPM-CFO materials. Antibacterial activity will be reviewed based on the percentage comparison of the area of the inhibition zone with the standard used.

**Characteristic of NPM-cobalt ferrite**

NPM-cobalt ferrite is one of the most commonly investigated magnetic spinel ferrites exhibiting such unique properties as hard magnetic material [14], high coercive field [12,15], high magnetostrictive [16], high magneto-crystalline anisotropy [7], chemical stability [18], moderate saturation magnetization [19,20], mechanical hardness [21], wear resistance and electrical insulation [22].

The structural formula of $CoFe_2O_4$ is $(Co_{1-i}^{2+}Fe_i^{3+})[Co_i^{2+}Fe_{2-i}^{3+}]O_4^{2-}$. The round and square brackets belong to tetrahedral and octahedral lattice sites, respectively [13]. Based on its distribution, cobalt ferrite belongs to the inverse spinel group where the divalent ion is in the octahedral site and the trivalent ion is distributed equally in the tetrahedral and octahedral sites [23]. The magnetic properties of NPM-CFO are considerably influenced by such factors as sample preparation and the synthesis method used [24,25], cobalt content [26], crystallite (particle) size [27], and cation distribution [28-32]. The synthesis method also has a considerable effect on cation distribution inside the lattice of cobalt ferrite [33,34].

Cobalt and iron oxides are desirable magnetic materials due to their specific properties and low-cost production. NPM-cobalt ferrite is a small-sized biocompatible device that can be assembled and lead to the advancement of cellular intake. The appropriate staying time and low dose in the patient body are interesting for *in vivo* applications of NPM-cobalt ferrite [35].

The ratio of surface area and volume causes the difference in surface atomic spins compared to the bulk ions due to the difference in the oxidation state. Spinel ferrites within the nano range have been investigated widely due to narrow size distribution and smaller particles possessing a larger surface area. The typical morphological characteristics of cobalt ferrite at the nanoscale are represented in **Figure 1**. **Figure 1** clearly shows that for NPM-cobalt ferrite, the TEM profile shows the presence of fine nano-grains. Then, the HR-TEM results show adjacent lines indicating the lattice parameter (*a*). It's hard work to achieve different properties for this material as morphology, size, and change of chemical composition. The effect of vacancies and the distribution of cations on properties like catalytic reaction is evident.

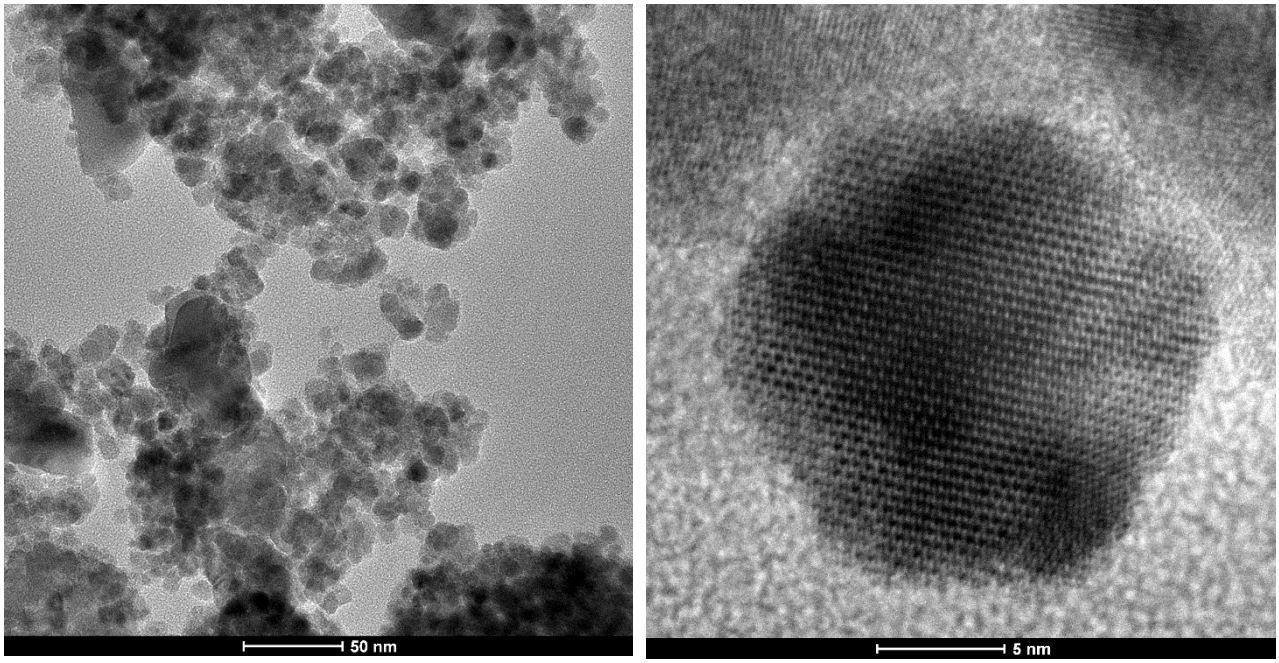


**Figure 1** Typical images of TEM and HR-TEM the NPM-cobalt ferrite.

**Synthesis of NPM-cobalt ferrite**

NPM-cobalt ferrite has been synthesized using various preparation techniques, such as microwave [36], thermal decomposition [37], solvothermal [38,39], sol-gel processing [40] and (auto) combustion [41], hydrothermal [42,43], co-precipitation [44-50], reverse co-precipitation [51], organic precursor decomposition [52], double sintering, citrate complex, mechanochemical synthesis, mechanical milling, sonochemical [38], microemulsion [53], solid state reaction [54], solid state combustion [55], and modified pechini [56].

The wet reaction material CFO includes a method with hydrothermal, microemulsion, sol-gel formation, and co-precipitation has been a popular method. At hydrothermal, the metallic nitrates are combined and added to distilled water, followed by treatment in autoclave and deposition of NPM-cobalt ferrite. At microemulsion, NPM-cobalt ferrite is formed in an emulsion using an appropriate surfactant, sol well prepared by polymerization or hydrolysis reactions via adding suitable reagents in the precursor solution, and the gelation process is conducted through polymers addition or sol condensation to gel [35]. In the sol-gel process, a hard porous gel is produced after a sol is created through hydrolysis and polymerization events. After that, the solvent and residuals are removed from the gel's pores by aging, drying, and annealing to produce the finished product. In the co-precipitation route, 2 solutions containing a precursor chemical are mixed, and then parameters like mixing rate, pH or temperature are changed to cause the precipitation of nanoparticles. The co-precipitation technique is reported to have advantages because it has been quite involved as a unique technique to prevent the agglomeration of nanoparticles (NPs) [57].

Recently, the use of natural materials to make environmentally friendly nanoparticles using green

synthesis methods has been widely developed. Some natural ingredients that have been used are lemon juice [56], rosemary extract [58], aloe vera [59], *Swertia chirata* extract [60], torajabin [61], sesame seed extract [62], *Salix alba* (white willow) [63], hibiscus extract [64], rooibos (*Aspalathus linearis*) tea [65], *Zingiber officinale* and *Elettaria cardamom* seed extracts [66], and *Tamarindus indica* fruit extract [67].

In addition to employing diverse techniques, there are other ways for investigation in the synthesis of NPM-CFO, including the employment of different fuels [68], variations in synthesis temperature, pH [69], molarity [70], chemical composition, and other factors. However, other post-synthesis treatments such as annealing temperature [71,72], annealing time [73], microwave treatment [74], and gamma irradiation [75] can also improve the performance of NPM-CFO. On the other hand, the preparation method is essential for studying antibacterial activity. Although the preparation method doesn't directly affect antibacterial performance, it does support the structural, morphological, and magnetic properties of the material, thus impacting its long-term antibacterial performance.

**The antibacterial mechanism of NPM-cobalt ferrite**

Most known that antibacterial activities of NPM-cobalt ferrite mainly depend on the reactive oxygen species (ROS) produced. It also depends on the size, morphology, surface area, increase in oxygen vacancies, chemical molecule diffusion ability, and the discharge of metal ions. The mechanisms of antibacterial activity in nanoparticles are adsorption, diffusion and antibiofilm [7].

Adsorption is the nanoparticle mechanism that adheres to the bacterial cell surface. The mechanism of transporting electrons and proteins is disrupted when bacterial cell walls absorb nanoparticles, which have a size comparable to that of a nanoscale particle. This causes membrane depolarization [76]. In the end, this mechanism may cause the death of bacterial cells.

The process of nanoparticles moving across a medium or bacterial environment is called diffusion. By this method, bacteria that are more widely distributed in the environment - such as those found in fluids or biofilms - can be reached by the nanoparticles. Smaller nanoparticles can diffuse more rapidly and effectively, opening up new possibilities for interactions with bacterial cells. Fenton reactions can arise from the release of metal ions by nanoparticles. Reactive oxygen radicals (ROS), which can damage cell membranes, break down DNA and proteins, and interfere with metabolic activities, are created via the Fenton reaction [7,77]. Additionally, the antibacterial mechanism of M-substituted NPM-cobalt ferrite is illustrated in **Figure 2**. First, the substituted metal ions are gradually released from the spinel lattice and interact with bacterial membrane components, disrupting the structural stability of the membrane. Second, the release of ions from the spinel ferrite enhances the surface redox reaction, leading to increased ROS generation. Finally, the combined effect of the cobalt ferrite properties and ROS attack then disrupts the membrane integrity, causing leakage of intracellular contents and ultimately resulting in bacterial inactivation.

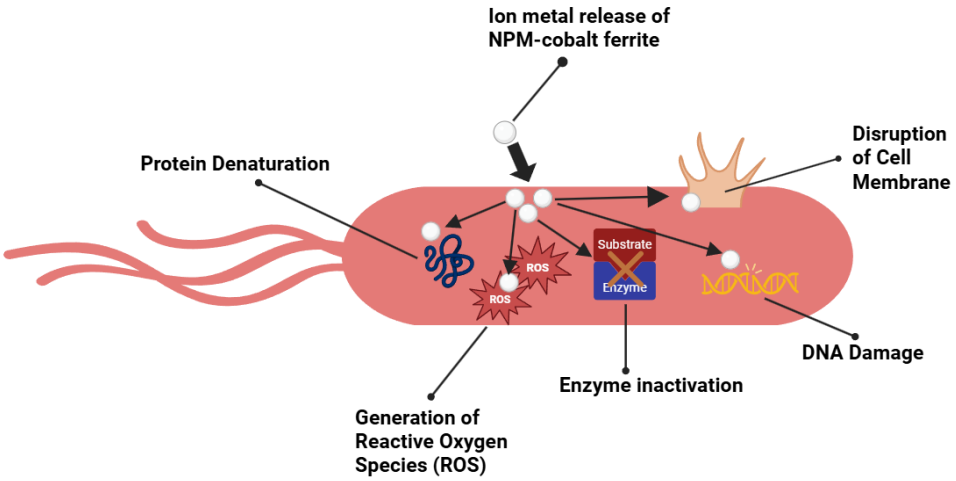


**Figure 2** Antibacterial mechanism of metal-substituted NPM-cobalt ferrite.

Moreover, antibiofilm functions by preventing or eliminating the development of biofilm, or protective layers. Antibiotics and other antibacterial drugs frequently cause biofilms to become extremely resistant. In order to prevent bacterial adherence, breach and harm the protective biofilm matrix, and prevent bacterial communication, nanoparticles adhere to the surface of bacteria [78].

Furthermore, lipoteichoic and trichoic acids are present in the peptidoglycan layer of Gram-positive bacteria. Gram-negative bacteria have an outer membrane made of protein, phospholipids, and lipopolysaccharides, as well as a thin coating of peptidoglycan. This leads to the conclusion that the resistance of the outer membrane envelope to reactive oxygen species produced on the photocatalytic surface as well as cell shape determine the rate of bacterial photoinactivation [79,80]. The all mechanism will produce clear zone of inhabitation (ZOI) as the result of antibacterial activity. Finally, the comparison of nanoparticle's area ZOI by standard is introduced for antibacterial performance as follows:

$$\text{Antibacterial Performance, AP (\%)} = \frac{\text{Surface area of ZOI (mm)}^2}{\text{Surface area of ZOI standard}^2} \times 100$$

**NPM-CFO as antibacterial agent**

Several papers have reported that NPM-cobalt ferrite has antibacterial properties. Below are various categories of NPM-cobalt ferrite compositions.

Aftab *et al.* [81] used solvothermal methods to manufacture a number of materials, including cobalt ferrite. X-ray diffraction study revealed that the crystallites' size was 5 nm, which is less than that of the other materials examined. The agar-well diffusion method was used to test its antibacterial efficacy against gram-positive *S. aureus* and gram-negative *E. coli*. Consequently, it was discovered that the nanomaterials' antibacterial activity depended on concentration. As concentration increased, the *S. aureus* bacterial zones of inhibition were found to be 0 and 11 mm, respectively. On the other hand, *E. coli* had a better inhibitory zone, measuring 4 and 12 mm with increasing concentrations. They came to the conclusion that there is a lot of promise for biomedical uses for nanoparticles as antibacterial agents.

Kaur *et al.* [81] fabricated magnetic heterocomposite of graphene supported $CoFe_2O_4/BiVO_4$ and explored the photocatalytic and antibacterial activities. The hydrothermal process was used in the fabrication of this material. Antimicrobial activity of $CoFe_2O_4/BiVO_4$ against *S. aureus* and *E. coli* was found to be good. It was discovered that as the concentration of *E. Coli* bacteria increased from 25 to 100 µg/mL, the inhibition zone increased from 11 to 20.5. In contrast, *S. aureus* bacteria's inhibitory zone very little changed as concentration increased.

Next, Shahriarinour *et al.* [83] also reported the antibacterial properties of magnetic cobalt ferrite nanoparticles. This material is synthesized using a one-step hydrothermal method of $Fe^{3+}$ to $Fe^{2+}$ with palm pollen suspension as a substrate and reducing agent. The particle size of date palm pollen loaded with cobalt ferrite magnetic nanoparticles (CFMNP-DPP) is around 19 nm, which is in line with the estimated particle size

from XRD data using the Scherrer method (20 nm). The magnetic intensity values were measured at 5 and 21 emu/g for cobalt ferrite nanoparticles which contained date palm pollen and those that did not. The coercive field of cobalt ferrite with date palm pollen, however, is higher than it is in the absence of date palm pollen. The antibacterial activity was studied using *Escherichia coli, Klebsiella pneumonia*, and *Staphylococcus aureus* bacteria with varying concentrations (10, 20, 30, 40, 50, 60 and 70 ppm). As a result, the zone of inhibition for all bacteria increased with increasing concentrations. The zone of inhibition is 6 - 10 mm for *E. coli*, 9 - 12 mm for *K. pneumonia*, and 7 - 11 mm for *S. aureus*. They concluded that the antibacterial properties of nanoparticles on *K. pneumonia* and *S. aureus* were higher than on *E. coli*. Differences in the antibacterial effects of nanoparticles against bacterial strains can be attributed to the nature of the amino acid residues used in their synthesis and differences in the structural composition of each bacterial culture.

El-khawaga *et al.* [84] promising photocatalytic and antimicrobial activity of novel capsaicin-coated cobalt ferrite nanocatalyst. Cobalt ferrite nanoparticles were prepared by the co-precipitation method and then surface modified with capsaicin. This material is confirmed to have grain sizes ranging between 15 and 25 nm for cobalt ferrite, while capsaicin-coated cobalt ferrite has a grain size ranging between 25 and 35 nm. Antimicrobial activity was tested on Gram-positive (*S. aureus*) and Gram-negative (*E. coli*) by the disk diffusion method. The inhibition zones for cobalt ferrite nanoparticles are 7.5 and 9.7 mm for *S. aureus* and *E. coli.* Meanwhile, the capsaicin-coated cobalt ferrite material has a larger inhibition zone, namely 23.5 and 17 mm for *S. aureus* and *E. coli*. Nanocomposites are more active against *S. aureus* than *E. coli*. This is influenced by the composition of the bacteria themselves; unlike Gram-positive bacteria, which combine a very compact form of peptidoglycan, the cell wall of Gram-negative bacteria consists of a layer of lipids, lipopolysaccharide, and peptidoglycan.

Manjunatha *et al.* [85] reported the effect of calcination temperature on the structural, antibacterial, radiation-shielding, and magnetic properties of cubic spinel cobalt ferrite. They claim that for the first time, cobalt ferrite nanoparticles were synthesized by the combustion method using *BigThyme* leaf extract as a reducing agent. The effect of the calcination temperature used was as follows: 200, 400, 600, and 800 °C. As a result, the crystal size increased from 12 - 79 nm with increasing calcination temperature. On the other hand, increasing the calcination temperature shows a soft ferromagnetic behavior with a high $M_s$ value (70.68 emu/g) and high coercive field (2.2 kOe). The antibacterial activity of the synthesized nanoparticles against Gram-positive (*Staphylococcus aureus*) and Gram-negative (*Escherichia coli*) pathogens was determined using the well diffusion method. Cobalt ferrite shows good sensitivity to gram-positive and gram-negative bacteria. However, the as-formed sample has a smaller zone of inhibition compared to calcined cobalt ferrite (800 °C). In *S. aureus* bacteria, there are inhibition zones of 52 and 38 mm, respectively, for the as-formed and 800 °C samples. Meanwhile, *E. coli* bacteria have a smaller inhibition zone than *S. aureus* bacteria at 25 and 19 mm, respectively, for as-formed and 800 °C sample.

Sulaiman *et al.* [82] reported the antibacterial activity of cobalt ferrite ($CoFe_2O_4$) nanoparticles against oral Enterococci. Cobalt ferrite is prepared using the sol-gel technique with sintering temperatures of 200, 400, and 600 °C. The crystal size from the calculation results was found to be 28.55 nm. The 600 °C sample has a coercive field value of 1,292.7 Oe and saturation magnetization of 91.6 emu/g. They reported that the magnetic moment of cobalt $Co^{2+}$ induces a large anisotropy that allows the magnetic nanoparticles to enhance biocompatibility and bacterial activity. Antibacterial activity revealed that the inhibition zone for pure cobalt ferrite nanoparticles (at temperatures of 400 and 600 °C) did not appear. However, an inhibition zone appeared when added with chlorhexidine (CHX) at 8.1 and 8.5, respectively, for nanoparticle samples at temperatures of 600 + CHX and 400 + CHX. Increased antimicrobial activity of chlorhexidine due to the increased surface-to-volume ratio of nanoparticles enhances interactions with bacteria. They state that precise control over nanoparticle size, shape, dispersion, and conditions influencing these properties are key requirements where special properties of nanoparticles are required for medical applications.

Suba *et al.* [83] made a nanocomposite of Apocynaceae leaf waste activated carbon (ALW) in combination with $CoFe_2O_4$ by an auto-combustion

method for antimicrobial activity. The crystallite size obtained was 10 nm. Evaluation of the magnetic properties of ALW/$CoFe_2O_4$ shows ferromagnetic behavior. The magnetization value obtained was 38.75 emu/g, which is lower than that of pure cobalt ferrite (94 emu/g). Meanwhile, the remanent magnetization and coercive field were obtained at 13.78 emu/g and 784.56 Oe. The antimicrobial activity of ALW/$CoFe_2O_4$ was tested by the well diffusion method. The synthesized nanocomposites were evaluated for their antimicrobial activity against *Staphylococcus aureus*, *Escherichia coli*, and *Candida ablicans* bacteria. As a result, there was an increase in the zone of inhibition for all bacteria with increasing concentrations (100, 200, 300, 400 and 500 mg/L). In *E. coli* bacteria, the inhibition zone is 10.5 - 17 mm, while in *S. aureus* and *C. albicans* bacteria, the inhibition zone is 11.83 - 17.5 and 11 - 17 mm. According to them, the antimicrobial potential of ALW/$CoFe_2O_4$ occurs through the electrostatic interaction of metal nanoparticles and microbial surfaces, which produces oxidative stress and DNA damage, which results in disruption of membrane function. Inactivation of bacterial enzymes by Co ions present in nanoclusters causes cell death.

Anusa *et al.* [84] investigated the structural comparison, optical properties, and antibacterial activity of cobalt ferrite with other materials. These nanoparticles were synthesized using the sol-gel method. The average crystallite size of cobalt ferrite nanoparticles has been calculated to be 35 nm, which is smaller than that of the reference material. Antibacterial activity was tested using *E. coli* and *S. aureus* bacteria. The inhibition zone for *E. coli* bacteria is 14 mm, while for *S. aureus* bacteria, there is no inhibition zone. Cobalt ferrite shows higher antibacterial activity on gram-negative bacteria than on gram-positive bacteria, which may be related to differences in cell wall structure.

Zachnowicz *et al.* [89] studied the structural, magnetic, cytotoxic, and antibacterial properties of polyrhodanine cobalt ferrite (PRHD@$CoFe_2O_4$) hybrid nanomaterials. Polymeric hybrid materials were synthesized via chemical oxidation polymerization. XRD analysis obtained a crystallite size of around 11 nm, which is in accordance with estimates using TEM analysis. Their analysis suggests changing the thickness of the PRHD layer can control the magnetic hardness and saturation magnetization of hybrid materials, which is attractive for biomedical applications. Antibacterial activity was tested using *E. coli* and *S. aureus* bacteria through *in vitro* assessment. Differences in composition ratios did not have a linear change in antibacterial activity. However, all samples showed prospective bactericidal properties against gram-positive and gram-negative bacteria. Polymeric shell thickness affected antimicrobial activity, reaching a critical value above which an increase in the amount of polymer did not influence activity. These results suggest that the investigated hybrid material may be a useful antimicrobial agent utilized for magnetic hyperthermia or magnetic carriers.

Sumathi *et al.* [85] synthesized NPM-cobalt ferrite using the co-precipitation method with a variety of precipitating agents, namely ammonium hydroxide, sodium hydroxide, and monoethanolamine. It was reported that different types of precipitating agents had an impact on the crystal size and antibacterial activity. The crystal sizes were found to range from 17 to 70 nm, obtained from the precipitating agent sodium hydroxide. Testing the antibacterial activity of the precipitating agent material, sodium hydroxide produced a higher antibacterial ratio (85%) against *S. aureus* than ammonium hydroxide (70%). The antibacterial mechanism is due to the hydrogen peroxide produced penetrating the cell wall and causing cell death. This penetration rate of hydrogen peroxide also plays a role in antibacterial activity. Thus, the antibacterial ratio depends on the various reagents used in the synthesis of NPM-cobalt ferrite.

**Table 1** Percentage of antibacterial activity in NPM-cobalt ferrite.

| Material | Method | *D* (nm) | *Ms* (emu/g) | *Hc* (Oe) | *Mr* (emu/g) | Microbial type | ZOI (mm) | AP (%) | Ref |
|---|---|---|---|---|---|---|---|---|---|
| CFO<br>Concentration: 500, 1,000 µg/mL | Solvothermal | 5 | - | - | - | *S. aureus*<br>*E. coli* | 0, 11<br>4, 12 | (0, 47.3)<br>(7.1, 64) | [86] |
| CFO/$BiVO_4$<br>Concentration (µg/mL): 25, 50, 100 | Hydrothermal | - | - | - | - | *E. coli*<br>*S. aureus* | (11, 16, 20.5)<br>(15.5, 15, 16) | (14.9, 31.52, 51.74)<br>(29.58, 27.7, 31.52) | [81] |
| CFO | One-step hydrothermal use date palm pollen | 20 | - | - | - | *E. coli*<br>*K.pnemonieae*<br>*S. aureus* | 6 - 10<br>9 - 12<br>7 - 11 | (8.2 - 22.7)<br>(16.7 - 29.8)<br>(12.3 - 30.3) | [87] |
| CFO<br>Composition: CFO, Capsaicin coated CFO | Co-precipitation | ~25<br>~35 | - | - | - | *S. aureus*<br>*E. coli* | 7.5, 9.7<br>23.5, 17 | (18.6, 69.9)<br>(182.4, 214.8) | [88] |
| CFO<br>Calcined: as-formed, 800 °C | Combustion use B*igThyme* leaf extract | 12 - 79 | 7.59 - 37.14 | 541.55 - 2,226.36 | 23.95 - 70.68 | *S. aureus*<br>*E. coli* | (38, 19)<br>(52, 25) | (124.9, 111.4)<br>(233.9, 192.9) | [89] |
| CFO<br>Sintering: 400 and 600 °C<br>with chlorhexidine | Sol-gel | 28.55 | 91.6 | 1292.7 | 49.9 | *Enterococci* | 8.5<br>8.1 | 32.1<br>29.2 | [82] |
| ALW/CFO | Auto combustion | 10 | 38.75 | 784.56 | 13.78 | *E. coli*<br>*S. aureus*<br>*C. ablicans* | 10.5 - 17<br>11.8 - 17.5<br>11 - 17.6 | 30.5 - 80<br>37.9 - 83.4<br>15.5 - 39.6 | [83] |
| CFO | Sol-gel | 35 | - | - | - | *E. coli*<br>*S. aureus* | 14<br>0 | 76.6<br>0 | [84] |
| PHRD@CFO<br>Amount of PHRD: 70, 210, 350, 700 | Chemical oxidation polymerization | 40 - 150 | ~25 - 110 | - | - | *E. coli*<br>*S. aureus* | 25, 26<br>29, 27<br>28, 25<br>28, 30 | (62.5k, 67.6k)<br>(84.1k, 72.9k)<br>(78.4k, 62.5k)<br>(78.4, 90k) | [90] |
| CFO<br>Precipitating agent: $NH_4OH$, NaOH | Co-precipitation | 70<br>17 | - | - | - | *S. aureus* | 10<br>5 | 8.2<br>2.0 | [85] |

**NPM-Metal-CFO applied for antibacterial**

Exploration of NPM-cobalt ferrite is increasingly varied, and the researchers report NPM- cobalt ferrite substituted with other elements (metal-CFO). The metals used are alkaline earth metals, transition metals, rare-earths and noble metals. Substitution can occur with Co ($M_xCo_xFe_2O_4$) or Fe ($M_xCoFe_{2-x}O_4$) depending on the cation number of each element which will affect the structural and magnetic properties of the nanoparticles. Several papers reveal the ZOI for pure CFO no zone [91-94], so that metal substitution in the CFO lattice becomes an interesting study to bring up or increase the bacterial inhibition zone. It is known that the release of metal ions allows to increase antibacterial activity.

**Alkaline earth metals**

***Magnesium***

There is very little substitution of cobalt ferrite with alkaline earth metals for antibacterial applications. Aisida *et al.* [95] synthesized Mg-substituted CFNPs using the sol-gel method.

They investigated the physical properties of antibacterial activity. The characterization results reveal that the crystal size of 40 nm is larger than that of pure cobalt ferrite at 31.3 nm. The particle size obtained is within the scope of the nanoparticle range for biomedical applications (100 nm magnification). By using the bacteria *Bacillus subtilis, Klebsiella pneumonia, Escherichia coli*, and *Staphylococcus epidermidis*, they looked at the susceptibility of the

samples to pathogenic strains through the inhibition zone. A higher IZ was found in *E. coli* bacteria (16 mm) compared to the positive control. They assume this is because gram-negative and gram-positive organisms have varying cell wall and membrane processes. CFNPs-substituted Mg samples were considered to have more potential as antibacterial agents compared to pure cobalt ferrite and cobalt ferrite-substituted Mn, which they also tested.

In another study, Mg metal was also substituted into cobalt ferrite to see its biomedical applications [96]. These nanoparticles are reported to have a date phase structure with a crystal size of 30.56 nm, smaller than pure cobalt ferrite of 48.08 nm. Antibacterial activity was tested using gram negative bacteria (*P. aeruginosa* and *E. coli*) and gram positive (*S. aureus*) with an incubation mass of 24 h. They reported that Mg substituted into cobalt ferrite showed responses against all pathogens tested. The results are not much different from pure cobalt ferrite (4.5 - 5.6 mm) and slightly lower (0 - 6.5 mm) than the co-doping also studied in their report. Mg-CFO has a minimum effect on *E. coli* bacteria.

**Table 2** Alkaline earth metals-CFO for antibacterial.

| Material | Method | *D* (nm) | *M*s (emu/g) | *H*c (Oe) | *M*r (emu/g) | Microbial type | ZOI (mm) | AP (%) | Ref |
|---|---|---|---|---|---|---|---|---|---|
| Mg-CFO | Sol-gel | 40 | - | - | - | *B. Subtilis* | 16 | 27.3 | [95] |
| | | | | | | *K. Pneumonia* | 16 | 24.2 | |
| | | | | | | *E. Coli* | 16 | 115.3 | |
| | | | | | | *S. Epidermis* | 11 | 64.5 | |
| Mg-CFO | Sol-gel | 48.08 | - | - | - | *P. aeruginosa* | 5.5 | 47.27 | [96] |
| | | | | | | *E. Coli* | 4.5 | 31.64 | |
| | | | | | | *S. aureus* | 5.4 | 45.56 | |

**Transition metals**

***Titanium***

Khalid *et al.* [97] have investigated titanium doped cobalt ferrite nanoparticles via the modified sol-gel method. Samples were prepared with the formula $CoTi_xFe_{2-x}O4$ where x = 0, 0.2, 0.4 and 0.6. They also produced $CoTi_{0.2}Fe_{1.8}O_4$/GO via a facile ultrasonication method. Antibacterial potential against *P. aeruginosa* and *S. aureus* was estimated from ZOI. The maximum ZOI was reported to be 52.3 mm in *P. aeruginosa* bacteria for nanocomposite material while the minimum ZOI of 12.4 mm was found in *S. aureus* bacteria for $CoTi_{0.6}Fe_{1.4}O_4$ nanoparticles. Titanium concentration has an inverse relationship with its antibacterial properties and is better against gram negative bacteria. This potential depends on the smaller size of the nanoparticles and the susceptibility due to the cell wall. In gram-negative bacteria, the peptidoglycan sheet is thinner which facilitates the diffusion of nanoparticles.

***Chromium***

Impact of Cr doping on the structural, surface morphology, magnetic properties and antibacterial activity of spinel nanoferrite ($CoFe_2O_4$) via sol-gel auto-combustion technique (SGACT) [97]. Samples are prepared with the formula $Cr_xCo_{1-x}Fe_2O_4$ where x = 0, 0.025, 0.05, 0.1, 0.15 and 0.20. Nanoparticles have a single phase for samples up to x = 0.05, while for x = 0.10 - 0.20 several additional phases of $Fe_2O_3$ are visible. They stated that with increasing Cr concentration the crystal size has an anomalous trend (range 40.49 - 44.26) which may be caused by the replacement of the smaller $Cr_{2+}$ ionic radius in place of $Co_{2+}$. Magnetic properties measurements reveal that the saturation magnetization decreases with increasing Cr ion concentration (0, 0.1 and 0.2). Antibacterial activity was tested using gram-positive (*S. aureus*) and gram-negative (*E. coli*) bacteria. In *E. coli* bacteria the maximum ZOI (17 mm) was found when doping Cr = 0.2 and the minimum (14.5 mm) when doping Cr x 0.05. Meanwhile, the *S. aureus* bacteria doping Cr x = 0.025 and 0.1 did not show an inhibition zone.

***Manganese***

Sanpo *et al.* [99] reported a 50% metal substitution synthesis on NPM-cobalt ferrites by the sol-gel synthesis method route using citric acid as a chelating. The composition was (a) $CoFe_2O_4$, (b) $Co_{0.5}Cu_{0.5}Fe_2O_4$, (c) $Co_{0.5}Zn_{0.5}Fe_2O_4$, (d) $Co_{0.5}Mn_{0.5}Fe_2O_4$ and (e) $Co_{0.5}Ni_{0.5}Fe_2O_4$. From the XRD results it is concluded that transition metals were completely substituted into the cobalt ferrite lattice. The crystallite size obtained are 42.97 ± 0.5, 40.14 ± 0.4, 44.18 ± 0.6, 40.26 ± 0.2 and 41.01 ± 0.5 nm, respectively. In the fundamental study, the XRD pattern results of NPM-cobalt ferrite substituted by transition metals are shown in **Figure 3(a)**. Furthermore, typical NPM-cobalt ferrite substituted with transition metal ions (Zn) is visualized using Vesta software (as shown in **Figure 3(b)**), which indicates that the cubic structure retains its crystal structure with the inclusion of Zn replacing Co in the cobalt ferrite structure. The antibacterial activity was obtained from (a) to (e) with the ZOI values respectively 42.97, 40.14, 44.18, 40.26 and 40.01 mm. The antibacterial properties of metal-cobalt ferrites are b > c > e > a > d. Therefore, it was concluded that based on the visualization of ZOI, the highest antibacterial property was (b) Cu-cobalt ferrite. In addition to the ZOI, typical SEM images representing the attached *S. aureus* and *E. coli* on synthesized transition metal-substituted cobalt ferrite nanoparticles are shown which look damaged by many dead bacteria.

Aisida *et al.* [95] have investigated the physical properties of cobalt ferrite nanoparticles doped with manganese for antibacterial activity. The crystal size of 23.7 nm is smaller than cobalt ferrite (31.3 nm) and other metal doping (40.9 nm). The prepared material showed the presence of an inhibitory zone which was tested on the 4 bacteria *Bacillus subtilis*, *Klebsiella pneumonia, Escherichia coli, Staphylococcus epidermis*. The highest zone of inhibition was found in *Klebsiella penumoniae* bacteria at 18 mm, followed by *Bascillus subtilis* (15 mm), *E. coli* (11 mm) and *Staphylococcus epidermis* (10 mm).

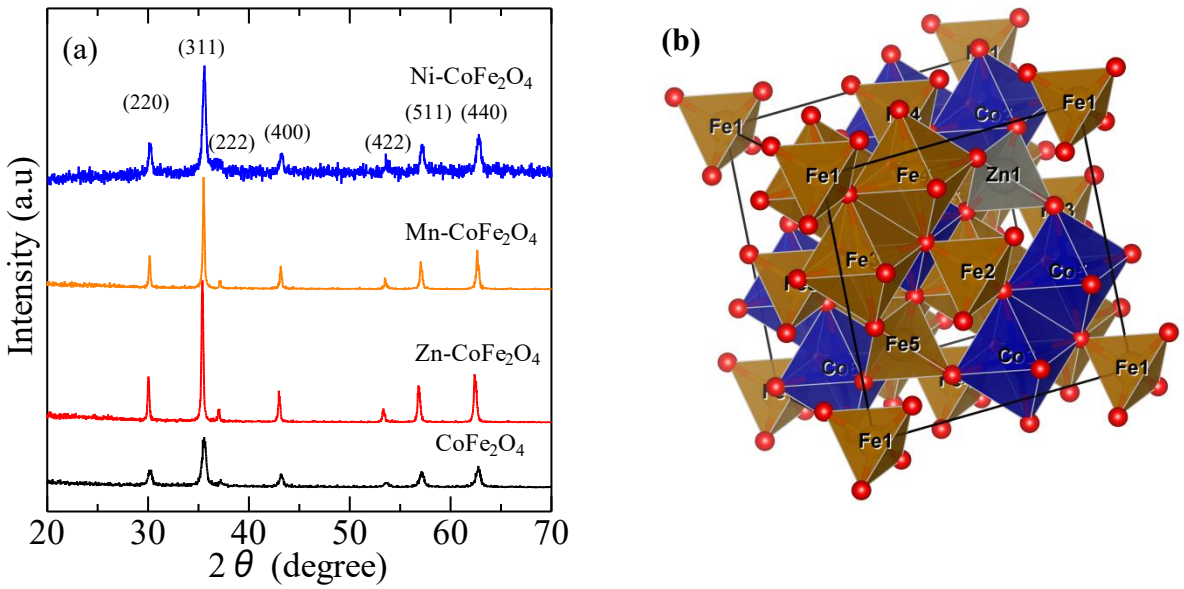


**Figure 3** (a) XRD pattern of metal transitions substituted NPM-cobalt ferrite and (b) Vesta visualization of Zn-$CoFe_2O_4$.

***Iron***

Zelnaravicius *et al.* [100] have investigated the substitution of Fe (II) into cobalt ferrite ferrite ($Co_xFe_{1-x}Fe_2O_4$, x = 0, 0.5 and 0.8) using the coprecipitation method. The cyst size varies from 3.1 - 3.8 nm. The smaller Fe doping concentration resulted in an increase in the antimicrobial potential to 93.1% - 86.3% for eukaryotic strains and to 96.4% - 42.7% for prokaryotic strains. This shows that pure cobalt ferrite has a higher antibacterial potential compared to the addition of Fe doping. This effect can be attributed to the determined higher positive Zeta potential values of pure cobalt ferrite than Fe(II)-doped ones in neutral and slightly acidic environments.

***Nickel***

Naik *et al.* [101] reported the multifunctional properties (one of which is antibacterial) of microwave-assisted bioengineered nickel-doped cobalt ferrite nanoparticles. Synthesis of nickel-doped cobalt ferrite nanoparticles using an extract from the *Andrographis paniculata* plant. The size of the crystallite decreases (From 32 to 24 nm) with increasing concentration of nickel. Its antibacterial activity was tested against gram-positive (*Staphylococcus aureus* and *Enterococcus faecalis*) and gram-negative (*Pseudomonas aeruginosa* and *Samonella typhi*) bacteria using the agar-well diffusion technique. The nanoparticle concentration was varied from 25 to 100 µg/mL. The report's findings demonstrated the antibacterial activity of nickel-cobalt ferrite nanoparticles against all strains and concentrations of bacteria. Both gram-positive and gram-negative bacteria have an expanded inhibitory zone in response to concentration increases. They discovered that the generation of reactive oxygen species (ROS) and the release of heavy metal ions are the primary factors influencing the produced nanomaterials' antibacterial activity effectiveness.

Sanpo *et al.* [99] have investigated the substitution of transition metals Cu, Zn, Mn and Ni in NPM-CFO synthesized via the sol gel route. Nickel doping is done with the composition $Co_{0.5}Ni_{0.5}Fe_2O_4$ producing a crystal size of 40.01 nm, which is the smallest size among other transition metal doping. All transition metal doping on CFO showed antibacterial activity on *E. coli* and *S. aureus* bacteria, where the ZOI on E. coli was greater than on S. aureus. Cu and Mn metal doping on NPM-CFO showed better antibacterial properties.

Kiani *et al.* [96] produced metal-doped cobalt ferrite via the sol-gel technique for biological applications. XRD examination verified the structure of the nanoparticles is single-phase; this is also validated by EDX. There is a decrease in the lattice constant with increasing Ni content caused by the smaller Ni ion radius (0.63 Å) replacing the cobalt ion site (0.78 Å). The average crystallite size decreases from 48.08 (undoped sample) to 29.47 nm with increasing Ni content. FTIR analysis results reveal the presence of 2 typical peaks, which are spinel phases, in all samples. Meanwhile, the particle shape is generally spherical (cubic) with some agglomeration between the particles. The average particle size was found to be 29 - 49 nm, which is close to the XRD calculation. The antibacterial properties of nickel cobalt ferrite were assessed using the disc diffusion method for common pathogens, namely Gram-negative (*Escherichia coli* and *Pseudomonas aeruginosa*) and Gram-positive (*Staphylococcus aureus*) bacteria. They revealed that nickel cobalt ferrite nanoparticles were active against S. *aureus* and *P. aeruginosa* bacteria with ZOI in the range of 4.5 - 5.6 mm. Meanwhile, no response was seen against *E. coli* bacteria.

***Zinc***

Zinc-substituted cobalt ferrite (Zn-CFO) nanoparticles with the formula $Co_{1-x}Zn_xFe_2O_4$ with (x = 0, 0.3, 0.5, 0.7 and 1) have been synthesized via the sol-gel method by Sanpo *et al.* [98]. It is reported that the crystal size of Zn-CFO ranges from (43 - 45) nm. Increasing the Zn concentration in cobalt ferrite significantly increased the antibacterial activity against *E. coli* and *S. aureus*. Meanwhile, the antibacterial activity against *E. coli* is higher than *S. aureus*. The possible mechanism for antibacterial activity is based on the main chemical species. Active oxide easily penetrates bacterial cell walls and causes cell damage, so the penetration rate of active oxide plays an important role in the rate of killing bacteria. Therefore, the antibacterial activity against *E. coli* and *S. aureus* obtained different results because the chemical composition of the cell walls is very different. In LB-agar plate assays, Zn-CFO nanopowders showed surface-dependent antibacterial activity.

Maksoud *et al.* [103] conducted antibacterial studies with Zn-CFO nanoparticles prepared using the sol gel method. The crystal size was found to be 12.86 nm. Several pathogenic microbes were used to test antibacterial activity with maximum growth inhibition results against *K. pneumoniae* bacteria (ZOI 28.00 mm). The inhibition zone for other pathogenic microbe ranges from (18 - 27) mm.

Another antibacterial study with NPM Zn-CFO was also carried out by Naik et al. with varying concentrations (x = 0, 0.2, 0.4 and 0.6) via the combustion method [99]. The crystal size decreased from 21 to 12 nm as the Zn concentration increased. Antibacterial activity was tested on gram-positive (*S. aureus*) and gram-negative (*S. typhi*) bacteria. The antibacterial activity on *S. typhi* from Zn-CFO showed a

high ZOI of 22 mm compared to pure CFO, namely 16 mm. In addition, increasing the mass concentration of nanoparticles (CFO and Zn-CFO) from 25 - 100 µg/mL was able to increase the ZOI value in both bacteria.

Iqbal *et al.* [105] reported the synthesis results of Zn-CFO with the composition $Zn_{0.5}Co_{0.5}Fe_2O_4$ which was prepared using the sol gel method. The average crystal size is 61.2 nm. NPM Zn-CFO has been proven to be able to inhibit the growth of *E. coli* and MRSA (Methicillin-resistant *Staphylococcus aureus*) bacteria. The zone of inhibition for MRSA (80%) is greater than for *E. coli* bacteria (69%). Meanwhile, increasing the incubation time (2, 4, 8, 21 and 24 h) resulted in a decrease in the ZOI growth of both bacteria.

Maksoud *et al.* [106] compared Zn, Cu, and Mn doping in cobalt ferrite ($M_xCo_{1-x}Fe_2O_4$, x = 0, 0.25, 0.5, 0.75) for antibacterial applications prepared via the sol gel method. Zn-CFO nanoparticles have a smaller crystal size, namely from 12.04 - 11.73 nm compared to other doping. Meanwhile, $Zn_{0.75}Co_{0.25}Fe_2O_4$ has an $M_s$ value of 68.42 emu/g (higher than other doping). Magnetic parameters are influenced by several factors such as homogeneity, porosity, density, morphology and arrangement of cations at lattice locations. The antibacterial test results showed that the composition $Zn_{0.75}Co_{0.25}Fe_2O_4$ had the best antibacterial activity in terms of the ZOI value against several bacteria tested. The largest ZOI was found in *S. aureus* bacteria (15.0 mm), followed by *E. columbae* bacteria (13.0 mm), and A. viridians (12.0 mm). The activity of $Zn_{0.75}Co_{0.25}Fe_2O_4$ may be related to the Debye temperature and rigidity of ferrite nanoparticles which increase antibacterial activity because bacteria diffuse into the holes of the synthesized ferrite nanoparticles.

**Table 3** NPM-cobalt ferrite doped transition metals for antibacterial.

| Material | Method | *D* (nm) | *M*s (emu/g) | *H*c (Oe) | *M*r (emu/g) | Microbial type | ZOI (mm) | AP (%) | Ref |
|---|---|---|---|---|---|---|---|---|---|
| Ti-CFO (x = 0.2, 0.4, 0.6) | Co-precipitation | 29 - 74 | - | - | - | *S. aureus*<br>*P. aeruginosa* | ~(34, 29, 18)<br>~(49, 35, 27) | ~(1,156, 841, 324)<br>~(1,067, 544.4, 324) | [100] |
| Cr-CFO x = 0, 0.025, 0.05, 0.1, 0.15, 0.2 | Sol-gel auto-combustion | 41.64<br>43.43<br>40.76<br>44.26<br>41.65<br>40.49 | 77.80<br><br><br>63.27<br><br>44.02 | 867<br><br><br>801<br><br>619 | 29.81<br><br><br>24.80<br><br>16.80 | <br><br>*S. aureus*<br>*E. coli*<br><br> | (0,0)<br>(0,0)<br>(12.5, 14.5)<br>(0,0)<br>(13.2, 0)<br>(13.8, 17) | (0, 0)<br>(0, 0)<br>(65, 61.4)<br>(0, 0)<br>(72.5, 0)<br>(79.3, 84.4) | [97] |
| (a) CoFe2O4, (b) Cu-CFO, (c) Zn-CFO, (d) Mn-CFO, (e) Ni-CFO | Sol-gel route using citric acid as a chelating agent | 42.97<br>40.14<br>44.18<br>40.26<br>40.01 | - | - | - | *E. coli*<br>*S. aureus* | b > c > e > a > d | - | [101] |
| CFO<br>Mn-CFO | Sol-gel | 31.3<br>23.7 | - | - | - | *B. Subtilis*<br>*K. Pneumonia*<br>*S. Epidermis*<br>*E. Coli* | 10,11,9,10<br>15,18,11,10 | (10.7, 11.5, 36.5, 53.3)<br>(24, 30.7, 54.5, 53.3) | [95] |
| Fe-CFO x = 0, 0.5, 0.8 | Co-precipitation | 3.8<br>3.1<br>3.6 | - | - | - | *C. albicans*<br>*C. parapsilosis*<br>*E. coli*<br>*S. aureus* | | (13, 6, 58, 4)<br>(11, 18, 70, 39)<br>(35, 20, 90, 75) | [102] |
| Ni-CFO x = 0, 0.25, 0.5, 0.75 concentration: 25, 50, 100 µg/mL | Microwave-assisted green route (*A. paniculata* extract) | 32<br>27<br>26<br>24 | - | - | - | *S. aureus*<br>*E. faecalis*<br>*P. aeruginosa*<br>*S. typhi* | 15, 22, 26<br>11, 16, 19<br>13, 18, 23<br>12, 17, 21 | (26.75, 57.55, 80.38)<br>(33.52, 70.91, 100)<br>(21.56, 41.33, 67.47)<br>(25, 50.17, 76.56) | [103] |
| Ni-CFO | Sol-gel | 40.01 | - | - | - | *E. coli*<br>*S. aureus* | | 70<br>95 | [101] |
| Ni-CFO x = 0, 0.25, 0.5 | Sol-gel | 48.08<br>42.48<br>29.47 | | | | *P. aeruginosa*<br>*E. coli*<br>*S. aureus* | (5.6, 4.5, 5.6)<br>0<br>(5.6, 4.5, 5.6) | (49, 31.6, 49)<br>0<br>(49, 31.6, 49) | [96] |
| Zn-CFO | Sol-gel | 44<br>43 | - | - | - | *E. coli*<br>*S.aureus* | | 50, 90<br>43, 83 | [98] |

| Material | Method | *D* (nm) | *Ms* (emu/g) | *Hc* (Oe) | *Mr* (emu/g) | Microbial type | ZOI (mm) | AP (%) | Ref |
|---|---|---|---|---|---|---|---|---|---|
| X = 0, 0.3, 0.5, 0.7, 1 | | 44<br>45<br>45 | | | | | | 40, 70<br>35, 62<br>30, 60 | |
| Zn-CFO | Sol-gel | 12.86 | - | - | - | *B. subtilis*<br>*K. pneumonia*<br>*P. aeruginosa*<br>*S.aureus*<br>*S. epidermis*<br>*A. baumannii*<br>*E. coli*<br>*E. faecalis*<br>*E. cloacae*<br>*C. albicans* | 26<br>28<br>27<br>26<br>25<br>23<br>27<br>27<br>19<br>18 | | [104] |
| Zn-CFO (Concentratio: 25, 50 and 100 µg | Combustion method using curd/cheese as a green fuel. | 12 - 18 | - | - | - | *S. aureus*<br>*S. typhi* | 4, 7<br>9, 12<br>15, 22 | 8.2, 19.1<br>41.3, 56.3<br>114.8, 189 | [99] |
| Zn- CFO Incubation time (2,4,8,21,24) | Sol-gel | 61.2 | 86.8 | 76.7 | 11.15 | MRSA<br>*E. coli* | | 80, 74, 75, 69, 64<br>69, 67, 55, 52, 47 | [105] |
| CFO<br>Zn-CFO<br>Cu-CFO<br>Mn-CFO<br>x = 0.25, 0.50, 0.75 | sol-gel method | 25.10<br>(12.04, 11.78, 11.73)<br>(12.10, 14.04, 13.78)<br>(15.68, 33.50, 27.84) | 68.419,<br>16.725,<br>28.821<br>53.929 | 34.01<br>109.53<br>1,617.30<br>344.01 | 34.014<br>1.307,<br>13.035<br>19.643 | *S. aureus,*<br>*Enterococcus*<br>*columbae, Aero*<br>*coccus viridians* | 0, 7, 8<br>15, 13, 12<br>12, 0, 10<br>11, 8, 8 | (0, 7.2, 27.3)<br>(40.4, 25, 61.5)<br>(25.9, 0, 42.7)<br>(21.7, 9.5, 27.3) | [106] |
| Bi-CFO | Combustion | - | - | - | - | *S. aureus*<br>*E. coli* | 20<br>23 | 156.3<br>313 | [107] |
| Bi-CFO (x = 0, 0.1) | Sol-gel combustion | ~54<br>~38 | - | - | - | *bacillus and coccus* | 8, 8.5<br>9, 9.5 | 64, 72.3<br>81, 90.3 | [108] |

**Post-transition metals**

***Stannum (Tin)***

Tin-doped cobalt ferrite nanoparticles were produced by Sobana et al. using the co-precipitation approach in order to study their magnetic and antibacterial characteristics [109]. An extract from the *Alfafa* plant was used in this synthesis (Lusan grass in north India). Consequently, the average crystallite size decreased from 39 to 22 nm with increasing Sn concentration (0, 0.2, 0.4, 0.6, 0.8 and 1.0). The production of an inverted spinel ferrite structure was also confirmed by Raman and FTIR. According to SEM and AFM studies, the surface had a uniform size distribution and was free of valleys. As the Sn concentration increased, the coercivity dropped from 960 to 470 G. They asserted that porosity, size distribution, magnetic particle shape, microstrain, magnetocrystallinity, and magnetic domain size are the primary parameters influencing coercivity. The antibacterial activity of undoped and Sn-doped cobalt ferrite was reviewed using *Escherichia coli* and *Bacillus subtilis* bacteria by the disc diffusion agar method. Compared to undoped cobalt ferrite, the zone of inhibition of Sn-doped cobalt ferrite was larger. They came to the conclusion that one of the main elements affecting antibacterial activity is particle size.

***Bismuth***

Kirankumar and Sumathi [107] used Bi ion doping and co-doping to investigate antibacterial activity. The nanoparticles were prepared using a combustion technique. The antibacterial test results showed that $Bi_{0.1}CoFe_{1.9}O_4$ nanoparticles were able to produce a greater ZOI than CFO, with a large ZOI for *S. aureus* bacteria (20 mm) and the ZOI for *E. coli* being 23 mm. Apart from that, they also added Cu ions to bismuth cobalt ferrite to form $Cu_{0.5}Co_{0.5}Fe_{1.9}Bi_{0.1}O_4$ which could increase the ZOI of 29 mm and 34 mm for the 2 bacteria tested. This confirms that metal substitution in CFO further increases antibacterial activity.

Another report regarding the antibacterial activity of Bi-CFO material was reported by Kalia *et al.* [108].

Cobalt ferrite was co-doped with bismuth and other metals of different concentrations via sol-gel combustion method. The crystallite sizes of these materials were ~54 nm for undoped and ~38 nm for doped Bi. Antibacterial activity was tested against bacillus and coccus bacteria using the disk diffusion method. There is an inhibition zone for both bacteria which shows antibacterial effectiveness. The Bi doped sample has an inhibition zone of 9 and 9.5 mm which is higher than the undoped sample.

**Table 4** NPM-cobalt ferrite doped post-transition metal for antibacterial.

| Material | Method | *D* (nm) | *M*s (emu/g) | *H*c (Oe) | *M*r (emu/g) | Microbial type | ZOI (mm) | AP (%) | Ref |
|---|---|---|---|---|---|---|---|---|---|
| Bi-CFO | Combustion | - | - | - | - | *S.aureus*<br>*E. coli* | 20<br>23 | 156.3<br>313 | [107] |
| Bi-CFO (x = 0, 0.1) | Sol-gel combustion | ~54<br>~38 | - | - | - | *bacillus and coccus* | 8, 8.5<br>9, 9.5 | 64, 72.3<br>81, 90.3 | [108] |

**Rare-earth metals**

***Cerium***

Ce substitution affects the structural, morphological, magnetic and antibacterial activity of cobalt ferrite nanoparticles prepared by the simple sol-gel combustion technique [110]. $CoCe_xFe_{2-x}O_4$ nanoparticles (x = 0, 0.1, 0.2, 0.3, 0.4 and 0.5) have a nano-sized single-phase cubic structure. The crystal size was reported to decrease from 25.36 to 16.53 nm with increasing cerium content. Ce substitution reduces the saturation magnetization of cobalt ferrite due to the substitution of $Ce^{3+}$ ion into the $Fe^{3+}$ ion site in site B. Meanwhile, the antibacterial activity is more dominantly influenced by the higher Ce content. They claim that the important role in antibacterial activity is the particle size and surface area of the sample.

***Neodymium & gadolinium***

Rehman *et al.* [111] have synthesized $CoNd_xFe_{2-x}O_4$ (x = 0.0, 0.1, 0.15 and 0.2) using sonochemical method. The crystal size obtained was 9 - 16 nm. Antibacterial activity was tested on *S. aureus*, *E. coli* and *C. albicans* bacteria. The Nd-CFO material showed higher antibacterial activity. Associated with particle size, it shows that increasing the surface to volume ratio of nanoparticles results in better antibacterial interactions.

Velho-Pereira *et al.* [111] compared doping (Bi, Gd, Nd) in cobalt ferrite CFO synthesized by the sol gel autocombustion method. Nd-CFO has the smallest crystal size, namely 4 nm compared to other doping. The antibacterial activity test with an incubation period of 24 h revealed that Nd-CFO had the highest antibacterial potential (83.73%) for *E. coli* (gram negative) bacteria. Meanwhile, the antibacterial activity for the gram-positive bacteria *S. epidermidis* was also high at 84.88% (lower than Bi doping 89.53%). These results show the ability of Nd-CFO to fight gram-positive and gram-negative bacteria because the 2 cell walls have different compositions. Gram-positive cell walls contain teichoic acid and murein, whereas gram-negative cell walls have lipid A, an LPS layer and a lower proportion of murein.

**Table 5** NPM-cobalt ferrite doped rare-earth metals for antibacterial.

| Material | Method | *D* (nm) | *M*s (emu/g) | *H*c (Oe) | *M*r (emu/g) | Microbial type | ZOI (mm) | AP (%) | Ref |
|---|---|---|---|---|---|---|---|---|---|
| Ce-CFO (x = 0.2, 0.3, 0.4 and 0.5) | Sol-gel - combustion | 20.98<br>19.85<br>18.67<br>16.53 | 47.87<br>38.35<br>35.46<br>29.32 | 95.47<br>93.92<br>91.95<br>89.48 | 9.94<br>8.91<br>7.45<br>5.98 | *Klebsiellapneumoniae*<br>*S. aureus* | 21, 20<br>23, 21<br>25, 19<br>27, 18 | (136.1, 123.5)<br>(163.3, 136.1)<br>(192.9, 111.4)<br>(225, 100) | [110] |
| Nd-CFO (x = 0, 0.1, 0.15 and 0.2) | Sonochemical | 9 - 16 | - | - | - | *S.aureus*<br>*C.albicans* | | (50, 45, 40, 30)<br>(9, 20, 22, 40) | [112] |

| Material | Method | *D* (nm) | *M*s (emu/g) | *H*c (Oe) | *M*r (emu/g) | Microbial type | ZOI (mm) | AP (%) | Ref |
|---|---|---|---|---|---|---|---|---|---|
| Gd-CFO | Sol-powder | 7 | - | - | - | *E. coli* | | 40, 70.93 | [111] |
| Nd-CFO | | 4 | | | | *S. epidermitis* | | 83.73, 84.88 | |

**Noble metals**

***Copper***

Sanpo *et al.* [113] substituted Cu in NPM-CFO via the sol-gel route, Cu-$CoFe_2O_4$ with various concentrations, namely 0, 0.3, 0.5, 0.7, and 1. The addition of $Cu^+$ ions reduced the average particle size from 41.52 to 37.54 nm. The lattice parameters also decrease with increasing Cu concentration, presumably because the ionic radius of $Cu^{2+}$ is smaller than $Co^{2+}$. The antibacterial test results showed that Cu-$CoFe_2O_4$ was able to inhibit the growth of *E. coli* and *S. aureus* bacteria. Increasing the concentration of Cu-$CoFe_2O_4$ increases the antibacterial effect on *S. aureus* while on *E. coli* bacteria it is consistent at around 45%. It was concluded that there are several factors that influence the level of bacterial killing such as crystal size, namely the surface to volume ratio, structure and chemical composition of the cell wall.

Prabagar *et al.* [114] investigated the effect of metal substitution (Cu, Zn, and Ag) in CFO. Synthesis was carried out using the sol gel auto combustion method with the composition $Co_{0.8}Cu_{0.2}Fe_2O_4$. The synthesis results show that the average crystal size of Cu-CFO is 18.89 nm, larger than pure CFO (13.50 nm). Magnetic studies show that the *M*s, *M*r and *H*c values for Cu-CFO are smaller than for pure CFO. The antimicrobial activity of Cu-CFO is most effective compared to pure CFO and other doping, because it has higher antimicrobial activity against selected pathogenic microbes. On the other hand, increasing the concentration of nanoparticles can increase the ZOI value of all doping ions.

***Argentum (Silver)***

Satheskumar *et al.* [115] carried out $Ag^+$ NPM-CFO ion doping with the chemical formula $Ag_xCo_{1-x}Fe_2O_4$ (x = 0 and 0.2), which was synthesized using honey assisted combustion. The secondary phase was found in Ag-$CoFe_2O_4$ nanoparticles which was caused by changes in the $Fe^{3+}$ and $O^{2-}$ environment in the spinel structure. The particle size of Ag-$CoFe_2O_4$ is 28.4 nm compared to $CoFe_2O_4$, which is 25.2 nm. The $Ag^+$ substitution also changes the magnetic properties of NPM-cobalt ferrites from the ferromagnetic order to the superparamagnetic order. This is thought to be caused by changes in particle size or anisotropic magnetocrystalline properties. The antibacterial activity of Ag-$CoFe_2O_4$ was better than $CoFe_2O_4$ against *E. coli* and *C. ablicans*. This better antibacterial activity is thought to be caused by the addition of $Ag^+$ ions which strengthen the process of cell distortion and death of bacterial species.

Mahajan *et al.* [116] substituted Ag+ into NPM-CFO with the composition $Ag_xCo_{1-x}Fe_2O_4$ (x = 0, 0.05, 0.01 and 0.02) using the sol gel auto-combustion method via chemical (citric acid) and green synthesis using tulsi extract seeds (*Ocimum sactum*) and garlic cloves (*Allium sativum*). These nanoparticles have a cubic structure (inverse spinel) with crystal sizes varying from 18 - 45 nm for different synthesis media. The magnetic characteristics of the Ms value were reported to be different, which was chemically mediated (49.95 emu/g), which used tulsi seeds extract (49.72 emu/g) and garlic cloves (28.89 emu/g). The Ag-CFO material was reported to be more effective as an antibacterial for gram-positive bacteria (*L. manocytagenes*) than for gram-negative bacteria (*E. coli*). The presence of $Ag^+$ ions in NPM-CFO causes an increase in ZOI because it is thought that $Ag^+$ ions induce the rate of oxygen oxidation on the surface of the species which will cause bacterial death.

In another study, Using the sol-gel process, Riyatun *et al.* [117] examined the actibacteria, magnetic properties, and microstructural features of silver-substituted cobalt ferrite nanoparticles. Ag concentrations of 0, 0.01, 0.02, 0.03, and 0.1 were employed. A concentration increase results in a 14 - 20.8 nm crystallite size increase. $Ag^+$ concentrations less than 0.03 suggest the absence of impurities or second phases, but $Ag_3O_4$ and $Fe_2O_3$ are the forms of other phases that emerge at doping levels of 0.1. When non-magnetic Ag ions are substituted, the magnetic characteristics alter.

The primary reason for the reduction in the coercive field is the substitution of non-magnetic $Ag^{+}$ for magnetic $Co^{2+}$. According to the findings of the study on antibacterial activity, every sample exhibited antibacterial activity against both gram-positive *S. aureus* and gram-negative *E. coli* bacteria. High $Ag^{+}$ doping (10%) indicates weaker antibacterial ability. The best antibacterial activity was found at 3% Ag doping, with an inhibition zone of 10.59 and 10.55 mm for *S. aureus* and *E. coli* bacteria, respectively.

Next, the structural, magnetic, and antibacterial characteristics of silver-substituted cobalt ferrite nanoparticles produced via the co-precipitation technique were found to be temperature dependent upon annealing by Riyatun *et al.* [113]. The physical properties were altered by applying an annealing temperature treatment of 200, 300, 400, and 500 °C. The annealing temperature increased, the crystallite size grew from 19.78 to 24.11 nm, and the grain size increased from 54.75 to 61.39 nm, according to XRD examination. Due to an increase in the magnetocrystalline anisotropy constant, an elevated annealing temperature results in an increase in the saturation magnetization and coercive field, which rise from 31.80 to 50.60 emu/g and 651 to 1.077 Oe, respectively. Using the well diffusion method, the antibacterial characteristics have been investigated with *S. aureus* and *E. coli*. The most notable for $Ag_{0.02}Co_{0.98}Fe_2O_4$ annealed at 200 °C with the minor grain size materials on *S. aureus* and *E. coli* were 12.73 mm (mortality of 88%) and 12.43 mm (mortality of 80%), respectively.

Riyatun *et al.* [119] also investigated nanoparticle preparation procedures to tailor the physical, antibacterial, and photocatalytic properties of silver-substituted cobalt ferrite. Co-precipitation and sol-gel techniques were used to create this material, with the synthesis temperature being changed to 70, 80, and 90 °C. Using both the sol-gel and co-precipitation techniques, it was discovered that the crystal size increased with increasing synthesis temperature. The crystal size of the co-precipitation technique is lower, ranging from 16.71 to 19.89 nm. The magnetic properties of silver cobalt ferrite also change with different preparation procedures. Compared to the co-precipitation approach, the coercive field of samples prepared by the sol-gel method has a higher value. Conversely, fluctuations in synthesis temperature and the saturation magnetization of samples prepared by the sol-gel technique exhibit a random magnitude, making the trend unpredictable. As the synthesis temperature rises, samples undergo an increase in the saturation magnetization value, in contrast to the co-precipitation approach. Using both the sol gel and co-precipitation procedures, the examination of antibacterial efficacy against gram-positive bacteria *S. aureus* and gram-negative bacteria *E. coli* revealed an increase in the inhibitory zone with increasing synthesis temperature. They came to the conclusion that antibacterial activity improved with increasing synthesis temperature. The sample at a synthesis temperature of 90 °C has the least specific surface area, however for antibacterial purposes, the material with the largest surface area to volume ratio is needed. The fact that the saturation magnetization of the nanoparticle sample increases as the synthesis temperature increases supports the idea that there is another mechanism - magnetic interaction - that leads to this.

Kalia *et al.* [108] researched the antibacterial activity of Ag-doped cobalt ferrite material and several other doped metals. When compared to the undoped sample (~54 nm), the crystal size of Ag-doped cobalt ferrite nanoparticles is reduced (~47 nm). Antibacterial activity was studied using the disc diffusion method against *Bacillus and Coccus* bacteria. For the examined microorganisms, the Ag-doped cobalt ferrite sample's zone of inhibition (ZOI) measures 8.5 and 9 mm, respectively. It was found that these outcomes were higher than those of undoped samples.

**Table 6** NPM-cobalt ferrite doped noble metals for antibacterial.

| Material | Method | *D* (nm) | *Ms* (emu/g) | *Hc* (Oe) | *Mr* (emu/g) | Microbial type | ZOI (mm) | AP (%) | Ref |
|---|---|---|---|---|---|---|---|---|---|
| Cu-CFO<br>x = 0, 0.3, 0.5, 0.7 and 1 | Sol-gel | 41.52<br>41.05<br>40.07 | - | - | - | *E. coli*<br>*S. aureus* | | 100, 100<br>59, 96<br>44, 87 | [114] |

| Material | Method | *D* (nm) | *Ms* (emu/g) | *Hc* (Oe) | *Mr* (emu/g) | Microbial type | ZOI (mm) | AP (%) | Ref |
|---|---|---|---|---|---|---|---|---|---|
| | | 38.97<br>37.54 | | | | | | 45, 72<br>44, 69<br>44, 58 | |
| Ag-CFO<br>Cu-CFO | Sol-gel auto combustion | 19.6<br>18.9 | 35.5<br>30.4 | 140<br>122 | 4.81<br>4.1 | *B. subtilis*<br>*Stahpylococcus*<br>*E. coli*<br>*K. Pnuemoniae*<br>*M. luteus*<br>*E. aerogenes* | 4,4,4,6,6,5<br>4,5,7,6,7,7 | (11.1,16,16,25, 36,14.8)<br>(11.1,25,49,25, 49,29) | [115] |
| Ag-CFO<br>x = 0, 0.2 | Honey assisted combustion | 40.9<br>39.2 | 60<br>38 | 1358<br>722 | 23.7<br>11.7 | *E. coli*<br>*S. aureus*<br>*C. ablicans* | 9.5,10,15<br>10.5,8.5,20.03 | (25.9,28.7,29.1)<br>(31.7,20,47.2) | [116] |
| Ag-CFO<br>(x = 0.005, 0.01 and 0.02)<br><br>T: Tulsi extract<br>G: Garlic extract | sol-gel auto-combustion technique using extract of tulsi seeds and garlic cloves | C = 23, 28, 30, 32<br>T = 18, 35, 40, 45<br>G = 22, 23, 27, 30 | 49.95<br>49.71<br>28.89 | 416. 34<br>280. 23<br>653. 25 | 19. 43<br>17. 43<br>10. 64 | *E. coli*<br>*monocytogenes* | C: 6,7,7, 8<br>T: 7,7,8,9<br>G: –, –, 5, 7<br><br>C: 7, 7, 8 ,9<br>T: 6, 7, 8, 9<br>G: –, 7, 8, 8 | | [117] |
| Ag-CFO<br>(x = 0, 0.01, 0.02, 0.03 and 0.1) | Sol-gel | 14.09<br>15.01<br>16.57<br>17.03<br>20.88 | 37.6<br>27.6<br>27.9<br>32<br>49 | 1,350<br>428<br>379<br>593<br>1,200 | 13.7<br>5.01<br>4.47<br>7.08<br>23.7 | *S. aureus*<br>*E. coli* | (10,10.06,10.34, 10.59,15.72)<br>(10,10.36,10.45, 10.55,13.27) | (13.1,13.3,14, 14.7,26.9)<br>(12.8,13.7,14, 14.2,21.3) | [118] |
| Ag-CFO<br>Annealing: 200, 300, 400 and 500 °C | Coprecipitation | 19.78<br>20.89<br>21.23<br>24.11 | 31.80<br>40.35<br>41.95<br>50.60 | 651<br>502<br>691<br>1,077 | 12.2<br>14.2<br>19.45<br>28.25 | *S. aureus*<br>*E. coli* | (12.73,13.14,11. 79,11.1)<br>(12.47,11.32,10. 96,11) | (17,18.1,14.5, 12.9)<br>(18.7,15.4, 14.4,14.5) | [113] |
| Ag-CFO<br>Synthesis temperature: 70, 80 and 90 °C | Sol-gel Coprecipitation | S: 19.88, 19.89,20.88<br>C: 16.71,18.98, 19.89 | S: 36.73, 58.36, 48.97<br>C: 50.60, 54.71, 56.95 | S: 1,350, 1,350, 1,200<br>C: 1,050, 1,200, 750 | S: 18.50, 30.18, 23.69<br>C: 24.50, 30.94, 28.31 | *S. aureus*<br><br>*E. coli* | S: 14.91, 15.45, 15.72<br>C: 13.84, 14.67, 15.20<br>S: 12,12.77, 13.27<br>C: 12.2, 13.65, 14.54 | (23.4,25.1,26)<br>(20.8,23.4, 25.1)<br><br>(17.4,19.7,21.3)<br>(18,22.5,25.6) | [119] |
| Ag-CFO<br>(x = 0, 0.1) | Sol-gel combustion | 54<br>47 | - | - | - | *bacillus and coccus* | 8, 8.5<br>8.5, 9 | 64, 72.3<br>72.3, 81 | [108] |

Hence, the comprehensive review and analytical assessment shown above indicate that substantial opportunities exist for future study directions, particularly in evaluating the stability of NPM–cobalt ferrite in biological environments. In addition, this study highlights the need to incorporate Antibacterial Performance (AP) as a complementary assessment parameter. AP can serve as a standardized justification metric linking physicochemical stability, ion-release behaviour, and reactive species generation to the actual biological efficacy of the material. On the other hand, incorporating AP into assessment frameworks in the next study on antibacterial applications would provide a more comprehensive and application-focused standard for evaluating the appropriateness of NPM-cobalt ferrite in biomedical technologies. Furthermore, current findings indicate that the antibacterial performance of these NPM-cobalt ferrite remains lower than that of commercial antibacterial agents. This gap highlights a key challenge for future studies, particularly the need to optimise ion-release behaviour, surface activity, and ROS generation to enhance their overall antibacterial potency. Overcoming these limitations is crucial to

advancing NPM-cobalt ferrite as a viable alternative to existing commercial agents.

## Conclusions

Metal substituted NPM-cobalt ferrite has emerged as a promising candidate for antibacterial applications due to its enhanced magnetic, structural, and biological properties. The antibacterial characteristics of the cobalt ferrite matrix are greatly enhanced by the addition of metal components, such as alkaline earth metals, transition metals, post-transition metals, rare earth metals, and noble metals. These dopants are efficient against different kinds of bacteria because they cause bacterial membrane rupture, reactive oxygen species (ROS) production, and disruption of microbial metabolic pathways. Nonetheless, there are still a lot of cobalt ferrite metals available that have antibacterial properties. Numerous aspects, such as the mass/concentration of the nanoparticles; the kind of bacteria utilized; the incubation duration; and crystallite, as well as particle size, surface area, and ion interactions of nanoparticles, all affect the bacterial inhibitory zone. The fact that so few metal alternatives have been employed indicates how much study remains to be done on the topic and how much promise there is for creating cobalt ferrite as an antibacterial material. This study's findings also demonstrated that ion substitution is a crucial component in the development of antibacterial activity, suggesting that using ions in place of other substances in cobalt ferrite nanoparticles may be a useful strategy for boosting antibacterial activity.

## Acknowledgements

This study was financially supported by Penguatan Kapasitas Grup Riset (PKGR-UNS) A contract number: 371/UN27.22/PT.01.03/2025.

## Declaration of Generative AI in Scientific Writing

The authors acknowledge the use of generative AI tools (Grammarly) in the preparation of this manuscript, specifically for language editing and grammar correction. No content generation or data interpretation was performed by AI. The authors take full responsibility for the content and conclusions of this work.

## CRediT author statement

**Retna Arilasita:** Data curation; Writing - Original draft preparation. **Nurdiyantoro Putra Prasetya:** Formal analysis; Writing - Review & Editing. **Utari:** Funding acquisition; Supervision. **Suharno:** Software; Data Curation. **Riyatun:** Methodology; Investigation. **Budi Purnama:** Conceptualization; Supervision, Writing - Review & Editing.

## References

[1] MS Alavijeh, MS Bani, I Rad, S Hatamie, MS Zomorod and M Haghpanahi. Antibacterial properties of ferrimagnetic and superparamagnetic nanoparticles: A comparative study. *Journal of Mechanical Science and Technology* 2021; **35(2)**, 815-821.

[2] M Saed, RD Ayivi, J Wei and SO Obare. Gold nanoparticles antibacterial activity: Does the surface matter? *Colloid and Interface Science Communications* 2024; **62** 100804.

[3] AS Hathout, A Aljawish, BA Sabry, AA El-Nekeety, MH Roby, NM Deraz, SE Aly and MA Abdel-Wahhab. Synthesis and characterization of cobalt ferrites nanoparticles with cytotoxic and antimicrobial properties. *Journal of Applied Pharmaceutical Science* 2017; **7**, 86-92.

[4] W Kachi, AM Al-Shammari and IG Zainal. Cobalt ferrite nanoparticles: Preparation, characterization and salinization with 3-aminopropyl triethoxysilane. *Energy Procedia* 2018; **157**, 1353-1365.

[5] M Barani, A Rahdar, M Mukhtar, S Razzaq, M Qindeel, SA Hosseini Olam, AC Paiva-Santos, N Ajalli, S Sargazi, D Balakrishnan, AK Gupta and S Pandey. Recent application of cobalt ferrite nanoparticles as a theranostic agent. *Materials Today Chemistry* 2022; **26**, 101015.

[6] RP Sharma, SD Raut, RM Mulani, AS Kadam and RS Mane. Sol-gel auto-combustion mediated cobalt ferrite nanoparticles: A potential material for antimicrobial applications. *International Nano Letters* 2019; **9**, 141-147.

[7] SV Gudkov, DE Burmistrov, DA Serov, MB Rebezov, AA Semenova and AB Lisitsyn. Do iron oxide nanoparticles have significant antibacterial properties? *Antibiotics* 2021; **10**, 1-23.

[8] YK Lakshmi, S Bharadwaj, S Chanda, CVK

Reddy, S Pola and KVS Kumar. Iron ion non-stoichiometry and its effect on structural, magnetic and dielectric properties of cobalt ferrites prepared using oxalate precursor method. *Materials Chemistry and Physics* 2023; **295**, 127172.

[9] NP Prasetya, R Arilasita, H Aldila, NA Wibowo, Riyatun, Utari, Nuryani, T Tanaka and B Purnama. Single-domain configuration tune high coercive field in Co-precipitated monazite-decorated cobalt ferrite nanoparticles. *Nano-Structures and Nano-Objects* 2024; **39**, 101301.

[10] PA Vinosha, A Manikandan, ASJ Ceicilia, A Dinesh, GF Nirmala, AC Preetha, Y Slimani, MA Almessiere, A Baykal and B Xavier. Review on recent advances of zinc substituted cobalt ferrite nanoparticles: Synthesis characterization and diverse applications. *Ceramics International* 2021; **47**, 10512-10535.

[11] H Kumar, A Giri and A Rai. Photocatalytic degradation of naphthol blue black dye using undoped and Al-doped cobalt ferrite nanoparticles. *Kuwait Journal of Science* 2024; **51**, 100208.

[12] H Nikmanesh, E Jaberolansar, P Kameli, GA Varzaneh, M Mehrabi, M Shamsodini, M Rostami, I Orue and V Chernenko. Structural features and temperature-dependent magnetic response of cobalt ferrite nanoparticle substituted with rare earth sm3+. *Journal of Magnetism and Magnetic Materials* 2022; **543**, 168664.

[13] X Jing, M Guo, Z Li, C Qin, Z Chen, Z Li and H Gong. Study on structure and magnetic properties of rare earth doped cobalt ferrite: The influence mechanism of different substitution positions. *Ceramics International* 2023; **49**, 14046-14056.

[14] SI Ahmad. Nano cobalt ferrites: Doping, structural, low-temperature, and room temperature magnetic and dielectric properties - A comprehensive review. *Journal of Magnetism and Magnetic Materials* 2022; **562**, 169840.

[15] R Dou, H Cheng, J Ma and S Komarneni. Manganese doped magnetic cobalt ferrite nanoparticles for dye degradation via a novel heterogeneous chemical catalysis. *Materials Chemistry and Physics* 2020; **240**, 122181.

[16] SD Bhame, A Bhapkar, MM Shirolkar and PA Joy. Magnetostriction studies on transition metal substituted cobalt ferrite. *Journal of the Indian Chemical Society* 2022; **99**, 100599.

[17] MS Al Maashani, KA Khalaf, AM Gismelseed and IA Al-Omari. The structural and magnetic properties of the nano-$CoFe_2O_4$ ferrite prepared by sol-gel auto-combustion technique. *Journal of Alloys and Compounds* 2020; **817**, 152786.

[18] A Chakrabarti, J Banerjee, S Chakravarty, S Samanta, M Nath, S Chattopadhyay, S Sarkar, SM Banerjee, S Chowdhury, SK Dash and A Bandyopadhyay. Exploration of structural and magnetic aspects of biocompatible cobalt ferrite nanoparticles with canted spin configuration and assessment of their selective anti-leukemic efficacy. *Journal of Magnetism and Magnetic Materials* 2022; **563**, 169957.

[19] S Mishra, SS Sahoo, AK Debnath, KP Muthe, N Das and P Parhi. Cobalt ferrite nanoparticles prepared by microwave hydrothermal synthesis and adsorption efficiency for organic dyes: Isotherms, thermodynamics and kinetic studies. *Advanced Powder Technology* 2020; **31**, 4552-4562.

[20] M Kaiser. Effect of silver nanoparticles on properties of cobalt ferrites. *Journal of Electronic Materials* 2020; **49**, 5053-5063.

[21] XB Xie, B Wang, Y Wang, C Ni, X Sun and W Du. Spinel structured $MFe_2O_4$ (M = Fe, Co, Ni, Mn, Zn) and their composites for microwave absorption: A review. *Chemical Engineering Journal* 2022; **428**, 131160

[22] A Maleki, N Hosseini and AR Taherizadeh. Synthesis and characterization of cobalt ferrite nanoparticles prepared by the glycine-nitrate process. *Ceramics International* 2018; **44**, 8576-8581.

[23] RK Kotnala and J Shah. *Ferrite materials: Nano to spintronics regime.* Elsevier, Amsterdam, Netherlands. 2015.

[24] M Houshiar, F Zebhi, ZJ Razi, A Alidoust and Z Askari. Synthesis of cobalt ferrite ($CoFe_2O_4$) nanoparticles using combustion, coprecipitation, and precipitation methods: A comparison study of size, structural, and magnetic properties. *Journal of Magnetism and Magnetic Materials* 2014; **371**, 43-48.

[25] DE Saputro, R Arilasita, Utari and B Purnama.

Tuning structural, magnetic and photocatalytic properties of bi-substituted cobalt ferrite nanoparticles. *Journal of Magnetics* 2021; **26**, 19-24.

[26] L Ajroudi, N Mliki, L Bessais, V Madigou, S Villain and C Leroux. Magnetic, electric and thermal properties of cobalt ferrite nanoparticles. *Materials Research Bulletin* 2014; **59**, 49-58.

[27] AL Gurgel, AE Martinelli, OLA Conceição, MM Xavier, MAM Torres and DMA Melo. Microwave-assisted hydrothermal synthesis and magnetic properties of nanostructured cobalt ferrite. *Journal of Alloys and Compounds* 2019; **799**, 36-42.

[28] NP Prasetya, RI Setiyani, Utari, K Kusumandari, Y Iriani, J Safani, A Taufiq, NA Wibowo, S Suharno and B Purnama. Cation trivalent tune of crystalline structure and magnetic properties in coprecipitated cobalt ferrite nanoparticles. *Materials Research Express* 2023; **10(3)**, 036102.

[29] S Sarmah, Aakansha, PK Maji, S Ravi and T Bora. Effect of cation distribution and temperature variation on magnetic and dielectric properties of manganese substituted cobalt ferrites. *Solid State Communications* 2021; **324**, 114146.

[30] B Purnama, AT Wijayanta and Suharyana. Effect of calcination temperature on structural and magnetic properties in cobalt ferrite nano particles. *Journal of King Saud University - Science* 2019; **31**, 956-960.

[31] AV Raut, DV Kurmude, SA Jadhav, DR Shengule and KM Jadhav. Effect of 100 kGy γ-irradiation on the structural, electrical and magnetic properties of $CoFe_2O_4$ NPs. *Journal of Alloys and Compounds* 2016; **676**, 326-336.

[32] R Kumar and M Kar. Lattice strain induced magnetism in substituted nanocrystalline cobalt ferrite. *Journal of Magnetism and Magnetic Materials* 2016; **416**, 335-341.

[33] C Dun, G Xi, X Heng, Y Zhang, Y Liu and X Xing. Comparative study on the magnetostrictive property of cobalt ferrite synthesized by different methods from spent Li-ion batteries. *Ceramics International* 2019; **45**, 8539-8545.

[34] Y Zhang, Z Yang, D Yin, Y Liu, C Fei, R Xiong, J Shi and G Yan. Composition and magnetic properties of cobalt ferrite nano-particles prepared by the co-precipitation method. *Journal of Magnetism and Magnetic Materials* 2010; **322**, 3470-3475.

[35] F Sharifianjazi, M Moradi, N Parvin, A Nemati, A Jafari Rad, N Sheysi, A Abouchenari, A Mohammadi, S Karbasi, Z Ahmadi, A Esmaeilkhanian, M Irani, A Pakseresht, S Sahmani and MS Asl. Magnetic $CoFe_2O_4$ nanoparticles doped with metal ions: A review. *Ceramics International* 2020; **46**, 18391-18412.

[36] IH Karakas. The effects of fuel type onto the structural, morphological, magnetic and photocatalytic properties of nanoparticles in the synthesis of cobalt ferrite nanoparticles with microwave assisted combustion method. *Ceramics International* 2021; **47**, 5597-5609.

[37] K Heydaryan, M Mohammadalizadeh, AH Montazer and MA Kashi. Reaction time-induced improvement in hyperthermia properties of cobalt ferrite nanoparticles with different sizes. *Materials Chemistry and Physics* 2023; **303**, 1-10.

[38] RS Yadav, I Kuřitka, J Vilcakova, J Havlica, L Kalina, P Urbánek, M Machovsky, D Skoda, M Masař and M Holek. Sonochemical synthesis of $Gd^{3+}$ doped $CoFe_2O_4$ spinel ferrite nanoparticles and its physical properties. *Ultrasonics Sonochemistry* 2018; **40**, 773-783.

[39] D Gheidari, M Mehrdad, S Maleki and S Hosseini. Synthesis and potent antimicrobial activity of $CoFe_2O_4$ nanoparticles under visible light. *Heliyon* 2020; **6,** e05058.

[40] J Venturini, AM Tonelli, TB Wermuth, RYS Zampiva, S Arcaro, ADC Viegas and CP Bergmann. Excess of cations in the sol-gel synthesis of cobalt ferrite ($CoFe_2O_4$): A pathway to switching the inversion degree of spinels. *Journal of Magnetism and Magnetic Materials* 2019; **482**, 1-8.

[41] S Dabagh and G Dini. Synthesis of silica-coated silver-cobalt ferrite nanoparticles for biomedical applications. *Journal of Superconductivity and Novel Magnetism* 2019; **32**, 3865-3872.

[42] Shyamaldas, M Bououdina and C Manoharan. Dependence of structure/morphology on electrical/magnetic properties of hydrothermally synthesised cobalt ferrite nanoparticles. *Journal of Magnetism and Magnetic Materials* 2020; **493**,

165703.

[43] MAM Khan, W Khan, M Ahamed, J Ahmed, MA Al-Gawati and AN Alhazaa. Silver-decorated cobalt ferrite nanoparticles anchored onto the graphene sheets as electrode materials for electrochemical and photocatalytic applications. *ACS Omega* 2020; **5**, 31076-31084.

[44] KC Nugroho, U Ubaidillah, R Arilasita, M Margono, BH Priyambodo, B Purnama, SA Mazlan and SB Choi. The effect of Sr-$CoFe_2O_4$ nanoparticles with different particles sized as additives in CIP-based magnetorheological fluid *Materials* 2021; **14(13)**, 3684.

[45] S Nasrin, FUZ Chowdhury and SM Hoque. Study of hyperthermia temperature of manganese-substituted cobalt nano ferrites prepared by chemical co-precipitation method for biomedical application. *Journal of Magnetism and Magnetic Materials* 2019; **479**, 126-134.

[46] EH El-Ghazzawy. Effect of heat treatment on structural, magnetic, elastic and optical properties of the co-precipitated $Co_{0.4}Sr_{0.6}Fe_2O_4$. *Journal of Magnetism and Magnetic Materials* 2020; **497**, 166017.

[47] M Arshad, M Asghar, M Junaid, MF Warsi, MN Rasheed, M Hashim, MA Al-Maghrabi and MA Khan. Structural and magnetic properties variation of manganese ferrites via Co-Ni substitution. *Journal of Magnetism and Magnetic Materials* 2019; **474**, 98-103.

[48] R Arilasita, Utari and B Purnama. Effect of low γ-irradiation dose the structural and the magnetic properties of Bi-substituted $CoFe_2O_4$ nanoparticles. *Journal of the Korean Physical Society* 2021; **79**, 185-190.

[49] DD Andhare, SR Patade, JS Kounsalye and KM Jadhav. Effect of Zn doping on structural, magnetic and optical properties of cobalt ferrite nanoparticles synthesized via co-precipitation method. *Physica B: Condensed Matter* 2020; **583**, 412051.

[50] M Kamran and M Anis-ur-Rehman. Enhanced transport properties in Ce doped cobalt ferrites nanoparticles for resistive RAM applications. *Journal of Alloys and Compounds* 2020; **822**, 153583.

[51] F Huixia, C Baiyi, Z Deyi, Z Jianqiang and T Lin. Preparation and characterization of the cobalt ferrite nano-particles by reverse coprecipitation. *Journal of Magnetism and Magnetic Materials* 2014; **356**, 68-72.

[52] T Tatarchuk, A Shyichuk, Z Sojka, J Gryboś, M Naushad, V Kotsyubynsky, M Kowalska, S Kwiatkowska-Marks and N Danyliuk. Green synthesis, structure, cations distribution and bonding characteristics of superparamagnetic cobalt-zinc ferrites nanoparticles for Pb(II) adsorption and magnetic hyperthermia applications. *Journal of Molecular Liquids* 2021; **328**, 115375.

[53] M Šuljagić, P Vulić, D Jeremić, V Pavlović, S Filipović, L Kilanski, S Lewinska, A Slawska-Waniewska, MR Milenković, AS Nikolić and L Andjelković. The influence of the starch coating on the magnetic properties of nanosized cobalt ferrites obtained by different synthetic methods. *Materials Research Bulletin* 2021; **134**, 111117.

[54] G Sharada, NP Kumar, P Sowjanya and D Sreenivasu. Low concentration doping effects of holmium on structural and spectroscopic properties of cobalt ferrite. *Materials Today: Proceedings* 2023; **92**, 440-444.

[55] A Lagashetty, A Pattar and SK Ganiger. Synthesis and characterization of Ag doped cobalt ferrite nanocomposite. *International Journal of Nano Dimension* 2019; **10**, 291-296.

[56] A Cheraghi, F Davar, M Homayoonfal and A Hojjati-Najafabadi. Effect of lemon juice on microstructure, phase changes, and magnetic performance of $CoFe_2O_4$ nanoparticles and their use on release of anti-cancer drugs. *Ceramics International* 2021; **47**, 20210-20219.

[57] SK Kulkarni. *Nanotechnology: Principles and practices.* 3rd ed. Springer, Switzerland, 2014.

[58] M Ghanbari, F Davar and AE Shalan. Effect of rosemary extract on the microstructure, phase evolution, and magnetic behavior of cobalt ferrite nanoparticles and its application on anti-cancer drug delivery. *Ceramics International* 2021; **47**, 9409-9417.

[59] N Dhanda, P Thakur and A Thakur. Green synthesis of cobalt ferrite: A study of structural and optical properties. *Materials Today: Proceedings* 2023; **73**, 237-240.

[60] S Fiaz, MN Ahmed, I ul Haq, SWA Shah and M Waseem. Green synthesis of cobalt ferrite and Mn doped cobalt ferrite nanoparticles: Anticancer, antidiabetic and antibacterial studies. *Journal of Trace Elements in Medicine and Biology* 2023; **80**, 127292.

[61] A Miri, M Sarani, A Najafidoust, M Mehrabani, FA Zadeh and RS Varma. Photocatalytic performance and cytotoxic activity of green-synthesized cobalt ferrite nanoparticles. *Materials Research Bulletin* 2022; **149**, 111706.

[62] D Gingasu, I Mindru, OC Mocioiu, S Preda, N Stanica, L Patron, A Ianculescu, O Oprea, S Nita, I Paraschiv, M Popa, C Saviuc, C Bleotu and MC Chifiriuc. Synthesis of nanocrystalline cobalt ferrite through soft chemistry methods: A green chemistry approach using sesame seed extract. *Materials Chemistry and Physics* 2016; **182**, 219-230.

[63] M Amiri, M Salavati-Niasari, A Akbari and T Gholami. Removal of malachite green (a toxic dye) from water by cobalt ferrite silica magnetic nanocomposite: Herbal and green sol-gel autocombustion synthesis. *International Journal of Hydrogen Energy* 2017; **42**, 24846-24860.

[64] D Gingasu, I Mindru, L Patron, JM Calderon-Moreno, OC Mocioiu, S Preda, N Stanica, S Nita, N Dobre, M Popa, G Gradisteanu and MC Chifiriuc. Green synthesis methods of $CoFe_2O_4$ and Ag-$CoFe_2O_4$ nanoparticles using hibiscus extracts and their antimicrobial potential. *Journal of Nanomaterials* 2016; **2016**, 2106756.

[65] MF Ayyıldız, DN Karaman, B Kartoğlu, M Şaylan, DS Chormey and S Bakırdere. A simple microwave-assisted synthesis of cobalt ferrite nanoparticles and its application for the determination of lead ions in rooibos (Aspalathus linearis) tea. *Food Chemistry* 2023; **429**, 136862.

[66] F Barkat, M Afzal, BS Khan, A Saeed, M Bashir, A Mukhtar, T Mehmood and K Wu. Formation mechanism and lattice parameter investigation for copper-substituted cobalt ferrites from *Zingiber officinale* and *Elettaria cardamom* seed extracts using biogenic route. *Materials* 2022; **15(13)**, 4374.

[67] D Gingasu, I Mindru, DC Culita, JM Calderon-Moreno, C Bartha, S Greculeasa, N Iacob, S Preda and O Oprea. Structural, morphological and magnetic investigations on cobalt ferrite nanoparticles obtained through green synthesis routes. *Applied Physics A: Materials Science and Processing* 2021; **127**, 1-14.

[68] VR Bhagwat, AV Humbe, SD More and KM Jadhav. Sol-gel auto combustion synthesis and characterizations of cobalt ferrite nanoparticles: Different fuels approach. *Materials Science and Engineering: B* 2019; **248**, 114388.

[69] DA Gole, SB Kapatkar, SN Mathad and RR Chavan. In vitro antimicrobial activity of cobalt ferrite nanoparticles synthesized by co-precipitation method. *Acta Chemica Iasi* 2020; **28**, 225-236.

[70] Suharyana, RR Febriani, NP Prasetya, Utari, NA Wibowo, Suharno, A Supriyanto, AH Ramelan and B Purnama. Sodium-hydroxide molarities influence the structural and magnetic properties of strontium-substituted cobalt ferrite nanoparticles produced via co-precipitation. *Kuwait Journal of Science* 2023; **50**, 575.

[71] A Chakrabarti, S Sarkar, BS Mitra, A Bandyopadhyay and S Chattopadhyay. Investigating the modification in structural properties of cobalt ferrite nanoparticles with increasing annealing temperature. *Materials Today: Proceedings* 2023. https://doi.org/10.1016/j.matpr.2023.05.006

[72] S Swathi, R Yuvakkumar, PS Kumar, G Ravi and D Velauthapillai. Annealing temperature effect on cobalt ferrite nanoparticles for photocatalytic degradation. *Chemosphere* 2021; **281**, 130903.

[73] CL Eduardo, EC Stockey, MF Ravanello, J Venturini, SZR Young, KMO Rubem, S Arcaro, BC Pérez and BS Roca. Correlation of synthesis parameters to the structural and magnetic properties of spinel cobalt ferrites ($CoFe_2O_4$) - An experimental and statistical study. *Journal of Magnetism and Magnetic Materials* 2022; **550**, 2-10.

[74] K Kombaiah, JJ Vijaya, LJ Kennedy, M Bououdina, RJ Ramalingam and HA Al-Lohedan. Okra extract-assisted green synthesis of $CoFe_2O_4$ nanoparticles and their optical, magnetic, and antimicrobial properties. *Materials Chemistry and Physics* 2018; **204**, 410.

[75] ESR El-Sayed, HK Abdelhakim and Z Zakaria. Extracellular biosynthesis of cobalt ferrite nanoparticles by *Monascus purpureus* and their antioxidant, anticancer and antimicrobial activities: Yield enhancement by gamma irradiation. *Materials Science and Engineering: C* 2020; **107**, 110318.

[76] H Namazi, M Pooresmaeil and R Salehi. Magnetic dialdehyde starch as green support for the growth of hyaluronic acid terminated covalent organic framework: A pH-controlled daunorubicin delivery system with inherent antibacterial feature. *European Polymer Journal* 2023; **198**, 112428.

[77] N Mammari, E Lamouroux, A Boudier and RE Duval. Current knowledge on the oxidative-stress-mediated antimicrobial properties of metal-based nanoparticles. *Microorganisms* 2022; **10(2)**, 437.

[78] W Li, W Wei, X Wu, Y Zhao and H Dai. The antibacterial and antibiofilm activities of mesoporous hollow $Fe_3O_4$ nanoparticles in an alternating magnetic field. *Biomaterials Science* 2020; **8(16)**, 4492-4507.

[79] A Mai-Prochnow, M Clauson, J Hong and AB Murphy. Gram positive and Gram negative bacteria differ in their sensitivity to cold plasma. *Scientific Reports* 2016; **6(1)**, 38610.

[80] L Pasquina-Lemonche, J Burns, RD Turner, S Kumar, R Tank, N Mullin, JS Wilson, B Chakrabarti, PA Bullough, SJ Foster and JK Hobbs. The architecture of the Gram-positive bacterial cell wall. *Nature* 2020; **582(7811)**, 294-297.

[81] K Aftab, T Naseem, S Hussain, S Haq, Mahfooz-ur-Rehman and M Waseem. Synthesis and characterization of $Ag_2O$, $CoFe_2O_4$, GO, and their ternary composite for antibacterial activity. *Environmental Science and Pollution Research* 2023; **30**, 4079-4093.

[82] M Kaur, M Dhiman, A Sudhaik, P Raizada, P Singh and S Gautam. Fabrication of magnetic heterocomposite of graphene supported $CoFe_2O_4$/$BiVO_4$ and exploration of photocatalytic and antibacterial activities. *Materials Today: Proceedings* 2023. https://doi.org/10.1016/j.matpr.2023.03.629

[83] M Shahriarinour, F Divsar, A Mehdipour, L Youseftabar-Miri and V Barkhordri. Antibacterial properties of cobalt ferrite magnetic nanoparticles loaded on date palm pollen against multidrug-resistant bacteria. *Arabian Journal for Science and Engineering* 2023; **48**, 7315-7322.

[84] AM El-Khawaga, MA Elsayed, YA Fahim and RE Shalaby. Promising photocatalytic and antimicrobial activity of novel capsaicin coated cobalt ferrite nanocatalyst. *Scientific Reports* 2023; **13**, 1-15.

[85] S Manjunatha, BC Reddy, HC Manjunatha, YS Vidya, KN Sridhar, L Seenappa, R Munirathnam, AN Santhosh, V Thirunavukkarasu, PSD Gupta, S Aluri, TYM Kumar, UM Pasha and MS Dharmaprakash. Effect of calcination temperature on structural, antibacterial, radiation shielding and magnetic properties of cubic spinel cobalt nanoferrite. *Materials Science and Engineering: B* 2022; **286**, 115978.

[86] JMA Sulaiman, SM Hamdoon and GY Abdulrahman. Antibacterial activity of cobalt ferrite ($CoFe_2O_4$) nanoparticles against oral enterococci. *Materials Science Forum* 2021; **1021**, 150.

[87] V Suba, G Rathika, KE Ranjith, M Saravanabhavan, VN Badavath and KS Thangamani. Enhanced adsorption and antimicrobial activity of fabricated Apocynaceae leaf waste activated carbon by cobalt ferrite nanoparticles for textile effluent treatment. *Journal of Inorganic and Organometallic Polymers and Materials* 2019; **29**, 550-563.

[88] R Anusa, C Ravichandran, TV Rajendran, MV Arularasu and EKT Sivakumar. Comparative investigation of cobalt ferrite ($CoFe_2O_4$) and cadmium ferrite ($CdFe_2O_4$) nanoparticles for the structural, optical properties and antibacterial activity. *Digest Journal of Nanomaterials and Biostructures* 2021; **14**, 367-374.

[89] E Zachanowicz, J Pigłowski, A Zięcina, K Rogacki, B Poźniak, M Tikhomirov, M Marędziak, K Marycz, J Kisała, K Hęclik and R Pązik. Polyrhodanine cobalt ferrite (PRHD@$CoFe_2O_4$) hybrid nanomaterials - Synthesis, structural, magnetic, cytotoxic and antibacterial properties. *Materials Chemistry and Physics* 2018; **217**, 553-561.

[90] S Sumathi, M Nehru and R Vidya. Synthesis,

characterization and effect of precipitating agent on the antibacterial properties of cobalt ferrite nanoparticles. *Transactions of the Indian Ceramic Society* 2015; **74**, 79-82.

[91] LTN Hoa, VN An, VHT My, PTT Giang, LK Top, HTC Nhan, PB Thang, TTT Van and LV Hieu. Silver decorated on cobalt ferrite nanoparticles as a reusable multifunctional catalyst for water treatment applications in non-radiation conditions. *RSC Advances* 2023; **13**, 24554-24564.

[92] AK Vishwakarma, BS Yadav, J Singh, S Sharma and N Kumar. Antibacterial activity of PANI coated $CoFe_2O_4$ nanocomposite for gram-positive and gram-negative bacterial strains. *Materials Today Communications* 2022; **31**, 103229.

[93] 371.AAG El-Shahawy, FIA El-Ela, NA Mohamed, ZE Eldine and WMA El Rouby. Synthesis and evaluation of layered double hydroxide/doxycycline and cobalt ferrite/chitosan nanohybrid efficacy on gram positive and gram negative bacteria. *Materials Science and Engineering: C* 2018; **91**, 361-371.

[94] M Kooti, P Kharazi and H Motamedi. Preparation, characterization, and antibacterial activity of $CoFe_2O_4$/polyaniline/Ag nanocomposite. *Journal of the Taiwan Institute of Chemical Engineers* 2014; **45**, 2698-2704.

[95] SO Aisida, K Ugwu, A Agbogu, I Ahmad, M Maaza and FI Ezema. Synthesis of intrinsic, Manganese and magnesium doped cobalt ferrite nanoparticles: Physical properties for antibacterial activities. *Hybrid Advances* 2023; **3**, 100049.

[96] MN Kiani, MS Butt, IH Gul, M Saleem, M Irfan, AH Baluch, MA Akram and MA Raza. Synthesis and characterization of cobalt-doped ferrites for biomedical applications. *ACS Omega* 2022; **8(4)**, 3755-3761.

[97] K Khalid, A Zahra, U Amara, M Khalid, M Hanif, M Aziz, K Mahmood, M Ajmal, M Asif, K Saeed, MF Qayyum and W Abbas. Titanium doped cobalt ferrite fabricated graphene oxide nanocomposite for efficient photocatalytic and antibacterial activities. *Chemosphere* 2023; **338**, 139531.

[98] S Kaur, VK Chalotra, R Jasrotia, V Bhasin, Suman, S Kumari, S Thakur, J Ahmed, A Mehtab, T Ahmad, R Singh and SK Godara. Spinel nanoferrite ($CoFe_2O_4$): The impact of Cr doping on its structural, surface morphology, magnetic, and antibacterial activity traits. *Optical Materials* 2022; **133**, 113026.

[99] N Sanpo, CC Berndt, C Wen and J Wang. Transition metal-substituted cobalt ferrite nanoparticles for biomedical applications. *Acta Biomaterialia* 2013; **9**, 5830-5837.

[100] R Žalnėravičius, A Paškevičius, K Mažeika and A Jagminas. Fe(II)-substituted cobalt ferrite nanoparticles against multidrug resistant microorganisms. *Applied Surface Science* 2018; **435**, 141.

[101] MM Naik, HSB Naik, N Kottam, M Vinuth, G Nagaraju and MC Prabhakara. Multifunctional properties of microwave-assisted bioengineered nickel doped cobalt ferrite nanoparticles. *Journal of Sol-Gel Science and Technology* 2019; **91**, 578-595.

[102] N Sanpo, J Wang and CC Berndt. Effect of zinc substitution on microstructure and antibacterial properties of cobalt ferrite nanopowders synthesized by sol-gel methods. *Advanced Materials Research* 2012; **535**, 436-439.

[103] MIA Abdel Maksoud, GS El-Sayyad, AH Ashour, AI El-Batal, MS Abd-Elmonem, HAM Hendawy, EK Abdel-Khalek, S Labib, E Abdeltwab and MM El-Okr. Synthesis and characterization of metals-substituted cobalt ferrite [Mx $Co_{(1-x)}Fe_2O_4$; (M = Zn, Cu and Mn; x = 0 and 0.5)] nanoparticles as antimicrobial agents and sensors for Anagrelide determination in biological samples. *Materials Science and Engineering: C* 2018; **92**, 644-656.

[104] NM Madhukara, NHS Bhojya, G Nagaraju, M Vinuth, K Vinu and R Viswanath. Green synthesis of zinc doped cobalt ferrite nanoparticles: Structural, optical, photocatalytic and antibacterial studies. *Nano-Structures & Nano-Objects* 2019; **19**, 100322.

[105] S Iqbal, M Fakhar-e-Alam, M Atif, N Amin, KS Alimgeer, A Ali, Aqrab-ul-Ahmad, A Hanif and FW Aslam. Structural, morphological, antimicrobial, and in vitro photodynamic therapeutic assessments of novel $Zn^{+2}$-substituted cobalt ferrite nanoparticles. *Results in Physics* 2019; **15**, 102529.

[106] MIAA Maksoud, GS El-Sayyad, AH Ashour, AI El-Batal, MA Elsayed, M Gobara, AM El-

Khawaga, EK Abdel-Khalek and MM El-Okr. Antibacterial, antibiofilm, and photocatalytic activities of metals-substituted spinel cobalt ferrite nanoparticles. *Microbial Pathogenesis* 2019; **127**, 144-158.

[107] VS Kirankumar and S Sumathi. Photocatalytic and antibacterial activity of bismuth and copper co-doped cobalt ferrite nanoparticles. *Journal of Materials Science: Materials in Electronics* 2018; **29**, 8738-8746.

[108] S Kalia, V Dhiman, CTT Tekou, D Basandrai and N Prasad. Antibacterial activities of Bi-Ag co-doped cobalt ferrite and their ZnO/Ag nanocomposite. *Inorganic Chemistry Communications* 2023; **150**, 110382.

[109] S Sobana, S Alagumanian, P Sakthivel and P Sivakumar. Characterization, magnetic and anti-bacterial properties of tin doped with cobalt ferrite nanoparticles prepared by co-precipitation technique. *International Journal of Research and Analytical Reviews* 2019; **6(1)**, 629.

[110] K Elayakumar, A Dinesh, A Manikandan, M Palanivelu, G Kavitha, S Prakash, KR Thilak, SK Jaganathan and A Baykal. Structural, morphological, enhanced magnetic properties and antibacterial bio-medical activity of rare earth element (REE) cerium ($Ce^{3+}$) doped $CoFe_2O_4$ nanoparticles. *Journal of Magnetism and Magnetic Materials* 2019; **476**, 157-165.

[111] S Rehman, MA Ansari, MA Alzohairy, MN Alomary, BR Jermy, R Shahzad, N Tashkandi and ZH Alsalem. Antibacterial and antifungal activity of novel synthesized neodymium-substituted cobalt ferrite nanoparticles for biomedical application. *Processes* 2019; **7(10)**, 714.

[112] S Velho-Pereira, A Noronha, A Mathias, R Zakane, V Naik, P Naik, AV Salker and SR Naik. Antibacterial action of doped $CoFe_2O_4$ nanocrystals on multidrug resistant bacterial strains. *Materials Science and Engineering: C* 2015; **52**, 282-287.

[113] N Sanpo, J Wang and CC Berndt. Sol-gel synthesized copper-substituted cobalt ferrite nanoparticles for biomedical applications. *Journal of Nano Research* 2013; **25**, 110-121.

[114] CJ Prabagar, S Anand, MA Janifer, S Pauline and PAS Theoder. Effect of metal substitution (Zn, Cu and Ag) in cobalt ferrite nanocrystallites for antibacterial activities. *Materials Today: Proceedings* 2021; **47**, 1999-2006.

[115] MK Satheeshkumar, ER Kumar, C Srinivas, N Suriyanarayanan, M Deepty, CL Prajapat, TVC Rao and DL Sastry. Study of structural, morphological and magnetic properties of Ag substituted cobalt ferrite nanoparticles prepared by honey assisted combustion method and evaluation of their antibacterial activity. *Journal of Magnetism and Magnetic Materials* 2019; **469**, 691-697.

[116] P Mahajan, A Sharma, B Kaur, N Goyal and S Gautam. Green synthesized (*Ocimum sanctum* and *Allium sativum*) Ag-doped cobalt ferrite nanoparticles for antibacterial application. *Vacuum* 2019; **161**, 389-397.

[117] R Riyatun, T Kusumaningsih, A Supriyanto and B Purnama. Characteristics of the microstructure, magnetic and antibacterial properties of silver-substituted cobalt ferrite nanoparticles from the sol-gel method. *Kuwait Journal of Science* 2023; **50**, 569-574.

[118] Riyatun, T Kusumaningsih, A Supriyanto and B Purnama. Temperature annealing dependence of structural, magnetic, and antibacterial properties of silver substituted cobalt ferrite nanoparticles produced by coprecipitation route. *Materials Research Express* 2023; **10(5)**, 056101.

[119] R Riyatun, T Kusumaningsih, A Supriyanto, HB Akmal, FM Zulhaina, NP Prasetya and B Purnama. Nanoparticle-preparation-procedure tune of physical, antibacterial, and photocatalyst properties on silver substituted cobalt ferrite. *Results in Engineering* 2023; **18**, 101085.